COMPARATIVE MODELING AND MOLECULAR DYNAMICS STUDIES ON TAR RNA BINDING PROPERTIES OF HUMAN IMMUNODEFICIENCY VIRUS TAT PROTEIN

A THESIS SUBMITTED IN PARTIAL FULFILLMENT

OF THE REQUIREMENTS FOR THE DEGREE OF

Master of Technology

In

Chemical Engineering

(Biochemical Engineering & Biotechnology)

By

SRIPAD CHANDAN PATNAIK

(ROLL NO. 20600001)

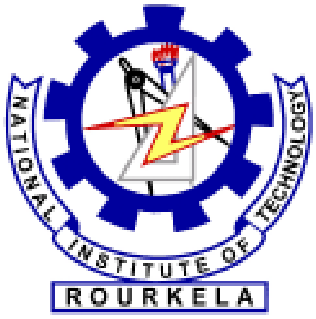

Department of Chemical Engineering

National Institute of Technology

Rourkela-769008, Orissa, India

2008

COMPARATIVE MODELING AND MOLECULAR DYNAMICS STUDIES ON TAR RNA BINDING PROPERTIES OF HUMAN IMMUNODEFICIENCY VIRUS TAT PROTEIN

A THESIS SUBMITTED IN PARTIAL FULFILLMENT

OF THE REQUIREMENTS FOR THE DEGREE OF

Master of Technology

In

Chemical Engineering

(Biochemical Engineering & Biotechnology)

By

SRIPAD CHANDAN PATNAIK

(ROLL NO. 20600001)

Under the Guidance of

Prof. Gyana R. Satpathy

Department of Biotechnology and Medical Engineering

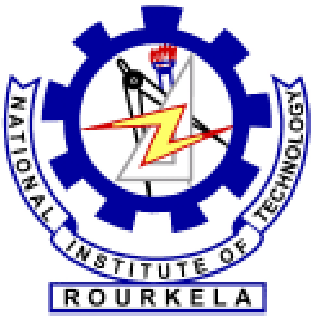

Department of Chemical Engineering

National Institute of Technology

Rourkela-769008, Orissa, India

2008

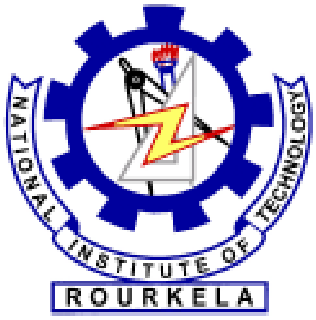

National Institute of Technology

Rourkela

CERTIFICATE

This is to certify that the thesis entitled, "Comparative modeling and molecular dynamics studies on TAR RNA binding properties of human immunodeficiency virus Tat protein" submitted by Sri Sripad Chandan Patnaik in partial fulfillment of the requirements for the award of Master of Technology in Chemical Engineering with specialization in "**Biochemical Engineering & Biotechnology**" at the National Institute of Technology, Rourkela (Deemed University) is an authentic work carried out by him under my supervision and guidance.

To the best of my knowledge, the matter embodied in the thesis has not been submitted to any other University / Institute for the award of any Degree or Diploma.

Date

Prof. Gyana R. Satpathy

Department of Biotechnology & Medical Engineering,

National Institute of Technology,

Rourkela –769008.

ACKNOWLEDGEMENT

I express my gratitude and deep regards to my guide Prof. Gyana Ranjan Satpathy for his valuable guidance, constant encouragement and kind co-operation throughout period of work which has been instrumental in the success of the dissertation. Thank you for your patience and understanding. I must also acknowledge our HOD, Dr. Kartik Chandra Biswal for giving this excellent opportunity to complete it successfully. I express my most sincere heartfelt gratitude to Dr. Subhankar Paul for his ready and able guidance for preparing the report.

Thanks to all my classmates for their love and support. I would like to thank my parents for supporting me to do complete my masters degree in all ways.

Sripad Chandan Patnaik

20600001

M.Tech.

----Contents----

Abstract

Macromolecules undergo changes with time and condition thereby affecting the structural and functional properties. These sequential and structural changes can be enumerated by comparative methods using the sequences and structural models. Molecular dynamics simulations are used to investigate dynamics and interactions of proteins in aqueous solution. We have studied the sequential variations in HIV-1 Trans-activating regulatory protein (Tat) among different strains and isolates taken from different geographical areas. Then these variations are modeled in consensus structures, so that each of the disparity can be suitably studied. Molecular dynamics simulation is carried out on each of these models to study the residual motions and interaction fluctuations. The results are compared and the functional implications of each of these transforms are studied. We have identified intra molecular interactions of importance for structure stabilization. The results show the functional characteristics of the protein or part of it is precisely reflected in its structural interactions and molecular dynamics flexibility.

Key words: Modeling, Molecular dynamics simulation, NAMD, Modeller, CHARMM, Tat, TAR RNA, Hydrogen interaction, RMSD.

LIST OF FIGURES

LIST OF TABLES

Chapter 1

1. Introduction

Human immunodeficiency virus (HIV) is a retrovirus that causes acquired immunodeficiency syndrome (AIDS). The life cycle of HIV inside the human host is complex and precise consisting many macromolecular interactions and activations. Each function is the window to next function performing role of molecular check point. Inhibiting one step effects the next impeding the cycle of viral replication and propagation [1]. One of such interaction between trans-activator of transcription (Tat) and transactivation responsive (TAR) region is responsible for initiation of transcription of viral RNA [2]. The interaction is vital for viral replication and propagation. The Tat protein suitably attaches itself to the TAR RNA hairpin structure to initiate the process. As the structural properties of the macromolecules involved guide the functional features carrying out the interaction, the three dimensional structure of both Tat and TAR is important for proper activation.

Macromolecules undergo changes with time and condition thereby affecting the structural and functional properties. The changes are due to various environmental conditions or process anomalies. These sequential and structural changes can be enumerated by comparative methods using the sequences and structural models. Molecular dynamics simulations are used to investigate dynamics and interactions of proteins in aqueous solution. We have considered the both of the above circumstances. First we have discussed the variability of the protein and incorporated these variabilities while modeling consensus structures based on a common template. In the second part we have done a dynamics study of these changes while keeping in mind the functional and conformational role they carry out in normal biochemical circumstances. In this way we have studied the importance of structural positions and their changes in a comparative manner.

HIV shows a high rate of variation in its genome. The virus differs significantly among its subgroups, generations, geographical area and with time. There is also a definite change in carrying out the function of the virus with these alterations. This is one of the major reasons for the failure of developing a drug against the HIV, as a drug effective for one group may not act against the other. Finding a constant feature both in macromolecular structure and life cycle of the virus is important for developing strategies

against the virus. The sequential and structural variations have to be studied for pointing out these constant features.

We have studied the sequential variations in HIV-1 TAR RNA element and Tat among different strains and isolates taken from different geographical areas. As the sequences are taken from different geographical areas they show variations in sequence and structure. Then these variations are modeled in consensus structures, so that each of the disparity can be suitably studied. Though the models are similar they differ in residues at important positions. Structures are compared at each segment and the structural aspect of each residual change is observed. Molecular dynamics simulation is carried out on each of these protein models to study the residual motions and interaction fluctuations with time. The results are compared and the functional implications of each of these transforms are studied. We have identified importance of intra molecular interactions for structure stabilization. The results show the functional characteristics of the protein or part of it are precisely reflected in its structural interactions and molecular dynamics flexibility.

Chapter 2

2. Literature review

2.1. Human immunodeficiency virus (HIV)

The first case of AIDS was first detected on June 5, 1981, when the U.S. Centers for Disease Control and Prevention reported a cluster of Pneumocystis pneumonia caused by a form of Pneumocystis carinii, now recognized as a distinct species Pneumocystis jirovecii, in five homosexual men in Los Angeles [3]. In 1982, the CDC introduced the term AIDS to describe the newly recognized syndrome.

In 1983, scientists led by Luc Montagnier at the Pasteur Institute in France first iosolated the virus that causes AIDS. They called it lymphadenopathy-associated virus (LAV) [4]. A year later a team led by Robert Gallo of the United States confirmed the discovery of the virus, but they renamed it human T lymphotropic virus type III (HTLV-III) [5]. In 1986 the virus was named human immunodeficiency virus (HIV) [6]. Infection with HIV occurs by the transfer of blood, semen, vaginal fluid, pre-ejaculate, or breast milk. Within these bodily fluids, HIV is present as both free virus particles and virus within infected immune cells. The three major routes of transmission are unprotected sexual intercourse, contaminated needles, and transmission from an infected mother to her baby at birth, or through breast milk [7].

HIV was classified as a member of the genus Lentivirus, part of the family of Retroviridae [8]. Lentiviruses have many common morphologies and biological properties. Many species are infected by lentiviruses, which are characteristically responsible for long-duration illnesses with a long incubation period. Lentiviruses are transmitted as single-stranded, positive-sense, enveloped RNA viruses. Upon entry of the target cell, the viral RNA genome is converted to double-stranded DNA by a virally encoded reverse transcriptase that is present in the virus particle. This viral DNA is then integrated into the cellular DNA by a virally encoded integrase so that the genome can be transcribed. Once the virus has infected the cell, two pathways are possible: either the virus becomes latent and the infected cell continues to function, or the virus becomes active and replicates, and a large number of virus particles are liberated that can then infect other cells [9].

HIV primarily infects vital cells in the human immune system such as helper T cells (specifically $CD4^+$ T cells), macrophages and dendritic cells. HIV infection leads to

low levels of $CD4^+$ T cells through three main mechanisms: firstly, direct viral killing of infected cells; secondly, increased rates of apoptosis in infected cells; and thirdly, killing of infected $CD4^+$ T cells by CD8 cytotoxic lymphocytes that recognize infected cells. When $CD4^+$ T cell numbers decline below a critical level, cell-mediated immunity is lost, and the body becomes progressively more susceptible to opportunistic infections. If untreated, eventually most HIV-infected individuals develop AIDS and die [10, 1, 7]. But the prognosis may be varied with viral starins.

2.1.1. Structure of the HIV

The virus is roughly spherical with spikes on the surface. The outer layer consists of the prospholipid viral envelope. Many copies of a complex HIV protein protrude through the surface of the virus particle. This protein, known as Env, consists of a cap made of three molecules called glycoprotein (gp) 120, and a stem consisting of three gp41 molecules that anchor the structure into the viral envelope. The underneath matrix layer consists up of protein p17. The inner capsid layer which encompasses the two positive single stranded RNA structures and enzymes such as reverse transcriptase, protease, integrase is made up of p24 proteins. The structure of the HIV is shown in Figure-1.

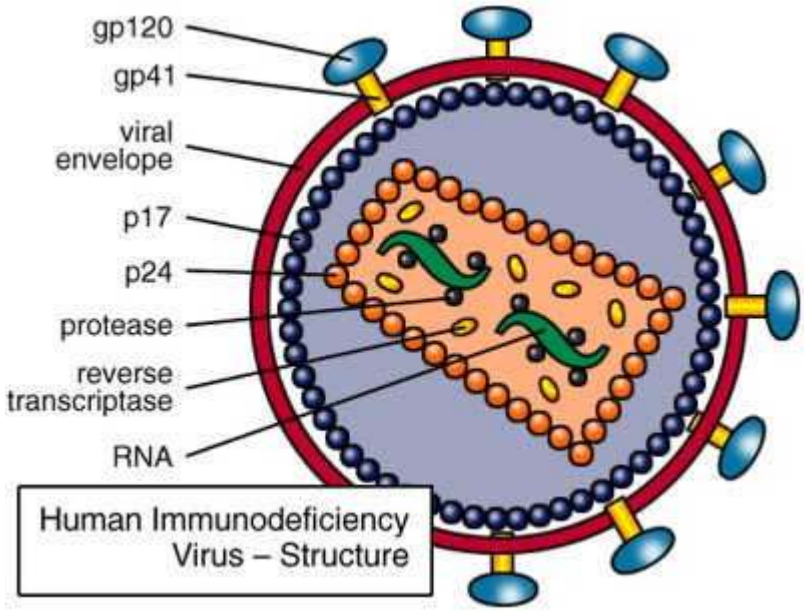

Figure-1: Structure of Human Immunodefficiency Virus

2.1.2. Genes

The HIV genome show nine genes and several structural elements. Out of these nine genes gag, pol, and env, contain information needed to make the structural proteins for new virus particles. The six remaining genes, tat, rev, nef, vif, vpr, and vpu (or vpx in the case of HIV-2), are regulatory genes for proteins that control viral replication and propagation [11]. The genetic organization of the virus is shown in figure-2.

The gag gene encodes the capsid proteins (group specific antigens). The precursor is the p55 myristylated protein, which is processed to p17 (Matrix), p24 (Capsid), p7 (NucleoCapsid), and p6 proteins, by the viral protease. Gag associates with the plasma membrane where the virus assembly takes place [12]. The pol genomic region encodes the viral enzymes protease, reverse transcriptase and integrase. These enzymes are produced as a Gag-Pol precursor polyprotein, which is processed by the viral protease [13]. The Gag-Pol precursor is produced by ribosome frameshifting near the 3' end of gag. The env genes give the proteins those are embedded in the outer layer of the virus. Viral glycoproteins produced as a precursor (gp160) which is processed to give a noncovalent complex of the external glycoprotein gp120 and the transmembrane glycoprotein gp41. gp120 contains the binding site for the CD4 receptor, and the seven trans-membrane domain chemokine receptors that serve as co-receptors for HIV-1 [14].

Tat is one of the two essential viral regulatory factors for HIV gene expression. Two forms are known, Tat-1 exon (minor form) of 72 amino acids and Tat-2 exon (major form) of 86 amino acids. Low levels of both proteins are found in persistently infected cells. Tat has been localized primarily in the nucleolus by immunofluorescence. It acts by binding to the TAR RNA element and activating transcription initiation and elongation from the LTR promoter, preventing the 5' LTR AATAAA polyadenylation signal from causing premature termination of transcription and polyadenylation. It is the first eukaryotic transcription factor known to interact with RNA rather than DNA and may have similarities with prokaryotic anti-termination factors. Extracellular Tat can be found and can be taken up by cells in culture [15]. Rev is the second necessary regulatory factor for HIV expression [16]. A 19 kD phosphoprotein, localized primarily in the nucleolus or nucleus, Rev acts by binding to RRE (Rev regulatory element) and promoting the nuclear export, stabilization and utilization of the viral mRNAs containing RRE. Rev is considered the most functionally conserved regulatory protein of

lentiviruses. Rev cycles rapidly between the nucleus and the cytoplasm. Viral infectivity factor (vif) is a basic protein of typically 23 kD. It promotes the infectivity but not the production of viral particles. In the absence of Vif the produced viral particles are defective, while the cell-to-cell transmission of virus is not affected significantly. Found in almost all lentiviruses, Vif is a cytoplasmic protein, existing in both a soluble cytosolic form and a membrane-associated form. The latter form of Vif is a peripheral membrane protein that is tightly associated with the cytoplasmic side of cellular membranes [17].

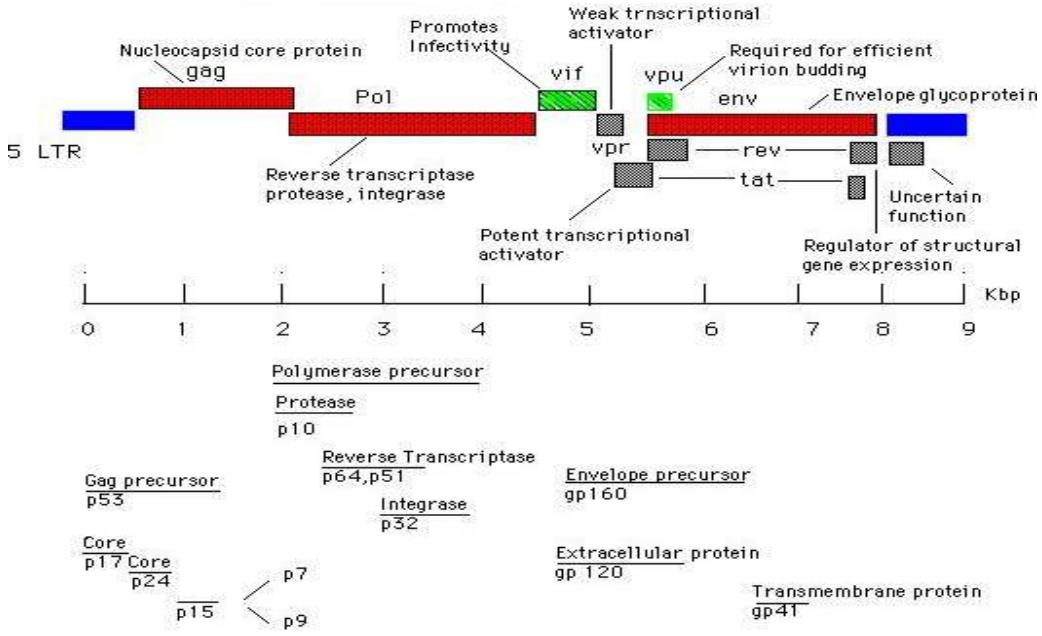

Figure-2: Genetic organization of HIV

Vpr (viral protein R) is a 96-amino acid (14 kD) protein, which is incorporated into the virion. It interacts with the p6 Gag part of the Pr55 Gag precursor. Vpr detected in the cell is localized to the nucleus. Proposed functions for Vpr include the targeting the nuclear import of preintegration complexes, cell growth arrest, transactivation of cellular genes, and induction of cellular differentiation. In HIV-2 and SIV the Vpx gene is apparently the result of a Vpr gene duplication. Vpu (viral protein U) is unique to HIV-1, SIVcpz. There is no similar gene in HIV-2. Vpu is a 16-kd (81-amino acid) type I integral membrane protein with at least two different biological functions: (a) degradation of CD4 in the endoplasmic reticulum, and (b) enhancement of virion release from the plasma membrane of HIV-1-infected cells [11]. Nef is a multifunctional 27-kd myristylated protein produced by an ORF located at the 3' end of the primate lentiviruses. Nef is

predominantly cytoplasmic. One of the first HIV proteins to be produced in infected cells; it is the most immunogenic of the accessory proteins. Nef is necessary for the maintenance of high virus load. Nef down regulates CD4, the primary viral receptor, and MHC class I molecules. It increases viral infectivity [18].

2.2. Genetic variability

Human immunodeficiency virus type 1 (HIV-1), which is a member of the Lentivirus genus (family Retroviridae), is characterized by a high level of genetic variation [19]. Members of Retroviridae are RNA viruses that replicate through a DNA intermediate. The viral RNA is copied into DNA by the viral enzyme reverse transcriptase. This process is quite error prone and forms the basis for the high genetic variability of these viruses. However, the observed genetic variation is a product of a complicated process influenced by many factors, most notably mutation and selection. The mutation rate of reverse transcriptase has been suggested to be 3.4 X 10^{25} mutations per base pair per replication cycle in vivo. In addition, the rate of genetic recombination in retroviruses is high, and this greatly contributes to the genetic variation. The apparent substitution rates across the genome are not the same, as illustrated by the presence of the five variable regions (V1 to V5) in the HIV-1 *env* gene [20].

Unlike bacterial genomes, the HIV-1 genome is A rich (36%) and C poor (18%). In vertebrates, the base composition varies between genes, and it has been suggested that the mosaic structure of the chromosomes reflects the varying G+C content [21]. Because of varying G+C content, the codon usage of a gene may vary with its genomic G+C context. It has been reported that HIV codon usage is dramatically different from that of cellular genes due to a high preference for A-rich codons and that this also results in a biased amino acid com-position of viral proteins. Furthermore, HIV-1 has been shown to produce extensive and monotonous G-to-A nucleotide substitutions, especially in the GpA dinucleotide. It has been suggested that a biased dCTP pool during reverse transcription is the cause of the G-to-A hyper mutation.

This variability is compounded when a single cell is simultaneously infected by two or more different strains of HIV. When simultaneous infection occurs, the genome of progeny virions may be composed of RNA strands from two different strains. This hybrid virion then infects a new cell where it undergoes replication. As this happens, the reverse transcriptase, by jumping back and forth between the two different RNA templates, will

generate a newly synthesized retroviral DNA sequence that is a recombinant between the two parental genomes. This recombination is most obvious when it occurs between subtypes [22].

Two species of HIV infect humans: HIV-1 and HIV-2. HIV-1 is thought to have originated in southern Cameroon after jumping from wild chimpanzees to humans. HIV-2 may have originated from the Sooty mangabeys, an old world monkey of Guinea-Bissau, Gabon, and Cameroon. HIV-1 is more virulent. It is easily transmitted and is the cause of the majority of HIV infections globally. HIV-2 is less transmittable and is largely confined to West Africa. HIV-1 is the virus that was initially discovered and termed LAV. The genetic sequence of HIV-2 is only partially homologous to HIV-1 and more closely resembles that of SIV than HIV-1 [7, 23].

2.3. Genomic diversity of clades

Three groups of HIV-1 have been identified on the basis of differences in env namely M, N, and O [24]. Group M is the most prevalent and is subdivided into eight subtypes (or clades), based on the whole genome, which are geographically distinct. The most prevalent are subtypes B (found mainly in North America and Europe), A and D (found mainly in Africa), and C (found mainly in Africa and Asia). These subtypes form branches in the phylogenetic tree representing the lineage of the M group of HIV-1.Co infection with distinct subtypes gives rise to circulating recombinant forms (CRFs) [25].

HIV-1 clades are phylogenetically classified on the basis of the 20–50% differences in envelope (env) nucleotide sequences. The Env proteins of groups M and O may differ by as much as 30–50% [26]. The N subtype, in turn, appears to be phylogenetically equidistant from M and O. Within M subgroups, inter-clade env variations differ by 20–30% whereas intra clade variation of 10–15% is observed. The pol region of HIV-1 is two to three times less divergent than env because this region encodes two critically important enzymes, reverse transcriptase and protease, which, if excessively mutated, render the virus inoperative. gag sequences are even further intolerant of mutations, seeing as they encode for relatively inflexible core protein sequences. Inter- and intra-clade variations within pol sequences are particularly relevant insofar as this region encodes reverse transcriptase and protease proteins, against which many antiviral drugs are directed. Variations in these regions may therefore affect drug susceptibility and development of drug resistance.

High degree of sequence variability is sufficient to alter the antigenic and biological properties of members of this virus group significantly [27]. The immunoreactive region of the gag protein is highly variable so that most epitopes are type-specific. This leads to a substantial reduction in the effectiveness of antibody assays based on this protein for serological diagnosis of infection with divergent HIV types. Variability in the envelope region is even greater so that neutralizing antibodies might be type-specific and allow multiple infections with different HIV variants in re-exposed individuals.

2.4. Drug and vaccine design

HIV differs from many other viruses as it has very high genetic variability. This diversity is a result of its fast replication cycle, with the generation of 10^9 to 10^{10} virions every day, coupled with a high mutation rate of approximately 3×10^{-5} per nucleotide base per cycle of replication and recombinogenic properties of reverse transcriptase. This complex scenario leads to the generation of many variants of HIV in a single infected patient in the course of one day. A significant challenge in the global effort to develop a vaccine against human immunodeficiency virus type 1 (HIV-1) is the extensive genetic variation observed among viral strains from different countries [28].

Many studies were performed to facilitate the design of an efficacious anti-HIV-1 vaccine by epitope based identification of CTL rich regions across HIV-1C Gag, Tat, Rev, and Nef [28, 29]. Hypothetically, an ideal HIV vaccine would contain multiple, highly responsive epitopes (CTL, T-helper, and neutralizing) derived from the locally circulating viral strains that cumulatively and complementarily would protect the host from HIV-1 infection, or, as a more realistic goal, could control HIV-1 infection, prevent progression to AIDS, and diminish HIV-1 transmission rate .

Phylogenetic analysis has shown that HIV-1 sequences can be classified into three main groups designated M, O, and N. Group M viruses are responsible for the majority of HIV-1 infections in the world and can be subdivided into subtypes A through D, F, G, H, J, K, and circulating recombinant forms (CRFs). Genetic subtypes show differences of as much as 24% in amino acid sequence, which raises the possibility that a vaccine candidate developed from one subtype may not be equally efficacious for other subtypes [30].

Elucidation of the phylogenetic origins of simian and human immunodeficiency viruses (SIV and LIV) is fundamental to the understanding of HIV pathogenesis and the spread of AIDS worldwide. Lentiviruses similar to human immunodeficiency viruses (HIVs) have been identified in a wide range of African primates including mangabeys (Cercocebus), guenons (Cercopithecus), mandrills (Papio) and chimpanzees (Pan) [31]. Although related to HIV in their physical structure, genetic composition and replicative properties, these simian immunodeficiency viruses SIV differ from the human AIDS viruses in one fundamental aspect of their biology: they fail to induce clinical immunodeficiency in their natural hosts. Understanding the molecular biology of these viruses, their lack of pathogenicity despite persistent replication and the processes responsible for their adaptation to a natural host may thus be important for achieving a better understanding of the virulence of HIV in man and the mechanisms underlying AIDS pathogenesis [32, 33].

Comparative analysis of TAR RNA structures in human and simian immunodeficiency viruses reveals the conservation of certain structural features despite the divergence in sequence [34]. Both the TAR elements of HIV-1 and SIV-chimpanzee can be folded into relatively simple one-stem hairpin structures. Chemical and RNAase probes were used to analyze the more complex structure of HIV-2 TAR RNA, which folds into a branched hairpin structure. A surprisingly similar RNA conformation can be proposed for SIV-mandrill, despite considerable divergence in nucleotide sequence. A third structural presentation of TAR sequences is seen for SIV-african green monkey. These results are generally consistent with the classification of HIV-SIV viruses in four subgroups based on sequence analyses (both nucleotide- and amino acid-sequences). However, some conserved TAR structures were detected for members of different virus subgroups. RNA structure analysis might provide an additional tool for determining phylogenetic relationships among the HIV-SIV viruses.

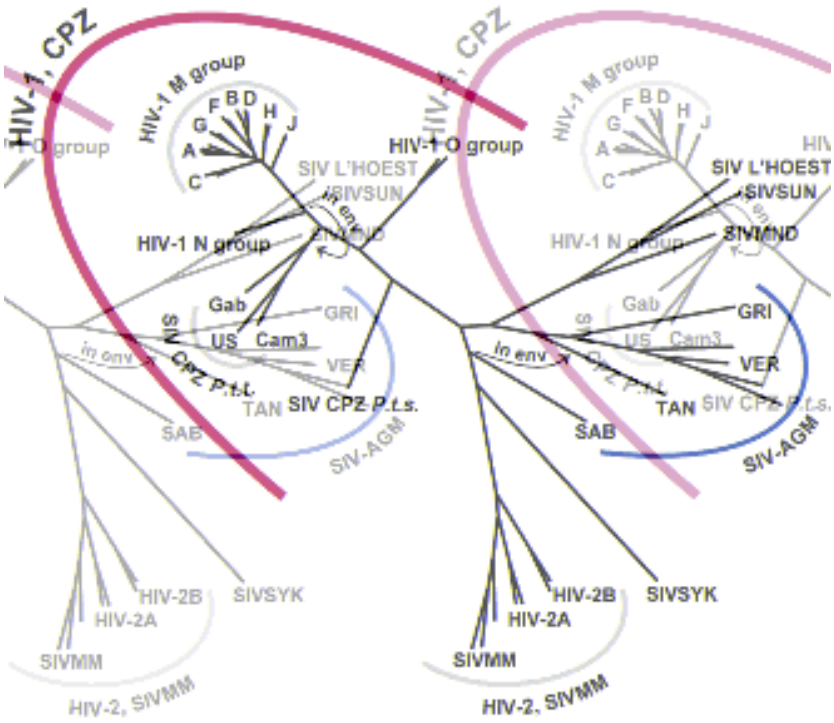

Figure-3: Phylogenetic Tree of the SIV and HIV viruses.

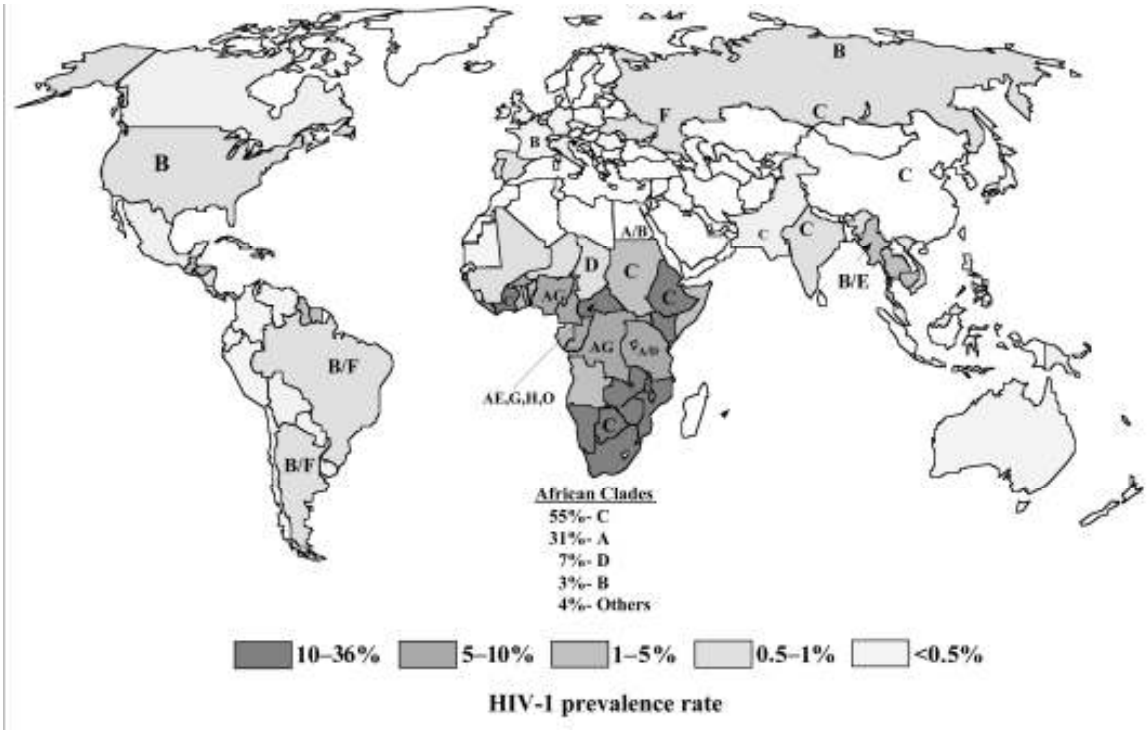

Figure-4: Subtype diversity of HIV-1 infections prevalent worldwide [27].

2.5. RNA Structure and Binding affinity

The functional diversity of RNA reflects diversity in its three-dimensional structure. Knowledge of the three-dimensional structures and general rules for RNA folding will be invaluable for deducing more detailed mechanisms of all RNA functions [35]. In the absence of high-resolution data, robust phylogenetic methods were developed to obtain secondary structure, and ingenious biochemical experiments were used to define nucleotide accessibility and to detect long range tertiary interactions [36]. RNA is nowadays the only molecule with the two properties of being a depository of genomic information with catalytic potential. Chemical catalysis requires a precise positioning of atoms in space and, therefore, RNA must achieve complex tertiary folds in order to reach transition states [37].

Binding of proteins and ligands to the RNA motif is purely based on the structure. Binding affinity of the components which defines stability of the complex is dependent on binding energy. This binding energy is a function of structure, charge and temperature (entropy). RNA sequences contain signatures specific for three dimensional motifs which participate in recognition and binding [38]. In regulatory pathways, RNA molecules exist in equilibria between transient structures differentially stabilized by effectors such as proteins or cofactors. Therefore, RNA molecules display their potential as drug targets on different levels, namely in three-dimensional folds, in structural equilibria and in RNA-protein interfaces [39].

The investigation of ligand-RNA interactions by computational approaches is dependent on the availability of three-dimensional models of RNA targets based on X-ray, NMR or phylogenetic data. Enormous progress in RNA synthesis and structure determination methods have helped to overcome many of the difficulties in obtaining NMR or crystal structures of RNA [40].

2.6. TAR-Tat interaction

The HIV trans-activating regulatory protein (Tat) protein carries out efficient transcriptional activation of viral long terminal repeat-linked genes by binding an RNA target structure termed TAR [1]. Tat-mediated trans-activation largely operates by increasing elongation efficiency of nascent transcripts or coordinating initiation and elongation from the HIV long terminal repeat (LTR). Presence of Tat protein is required for the total transcription, in the absence of which the short transcripts predominates [2,

41]. Deletion analysis of the viral LTR showed that the genetic element responsible for Tat activity, the trans-activation responsive region (TAR), is generally located downstream of the initiation site for transcription nucleotides +1 and +59 [15]. It also interacts with the Cyclin T1 (CycT1) subunit of the positive transcription elongation factor complex, P-TEFb inducing co-operative binding of the P-TEFb complex onto nascent HIV-1 TAR RNA [42].

The simplest explanation for the nature of Tat to activate transcription from viral LTRs that carry TAR elements is that Tat binds directly to TAR RNA. After purification of recombinant Tat it is demonstrated that it is able to specially recognize TAR RNA [43]. Subsequently, it was noted that synthetic peptides carrying the basic domain of Tat are also able to bind directly to TAR RNA [44].

Despite extensive efforts, the crystals of HIV-1 Tat have not been obtained [15]. The best information about the three-dimensional structure of Tat is based on nuclear magnetic resonance (NMR) [45, 46]. The Tat sequence can be subdivided into several distinct regions on the basis of its amino acid composition and the nature of its role in basic function [47, 48]: a N-terminal activation region (NT, amino acids 1–19), a cysteine-rich core domain (CRD, amino acids 20–31), a core region (amino acids 32–47), a arginine rich RNA binding domain (ARD, amino acids 48-57), a glutamine-rich region (QRD, amino acids 58–76) and the C-terminal (CT, amino acids 77-86).

The RNA binding property is clearly reflected in the structure of Tat protein. The core, basic and glutamine rich region are all involved in RNA binding. The recent NMR studies of HIV [47] and equine infectious anemia virus (EIAV) [49] Tat proteins show a compact core structure and the close proximity between the N terminus and the basic region. Addition of the core region of Tat to basic polypeptide mimics of Tat leads to enhanced binding and a considerable improvement in the quality of the NMR spectra [48]. This shows the binding affinity of Tat protein and in particular the basic region towards the TAR RNA.

Binding is mediated by a ten amino acid basic domain that is rich in arginine and lysines [50]. Circular dichroism and two-dimensional proton NMR studies of this hybrid peptide indicate that the Tat basic domain forms a stable α-helix, whereas the adjacent regulatory sequence is mostly in extended form. These findings suggest that the tendency

to form stable α-helices may be a common property of arginine and lysine rich RNA binding domains [51].

Interactions and participating macromolecules undergo modification in relation to time, condition and genomic strength of the organism [52]. Enumerating characteristics and attributes to quantify these modifications is essential for quantifying these changes, both structural and functional. Mathematical and computational tools can be useful for analyzing these changes in interaction and its effect on viral lifecycle. Molecular dynamics simulation is used in various studies to find out structural [54], binding [56, 99, 100] and functional properties of various systems like protein [54, 98], protein-ligand complex [99, 56] and membrane molecules [96, 97]. Molecular dynamics is used in defining the binding pathways of proteins with other macro molecules [101, 102]. Similarly several dynamics studies have been done taking Tat protein alone or complex with TAR RNA element or other macromolecules [53, 54]. The studies show the dynamics and intermolecular interaction among the different region of the protein [54]. These studies also demonstrate the relationship between the residual motion and functional role of the residue. The molecular dynamics study also shows the flexibility of both TAR RNA and basic arginine rich peptide while forming a complex [55, 56]. An interdomain motion is observed in the simulation of free TAR, which is absent in the case of bound TAR, leading to the conclusion that the free conformation of TAR is intrinsically more flexible than the bound conformation. Free energy analysis, which includes salvation contributions, was used to evaluate the influence of van der Waals and electrostatic terms on formation of the complex and on the conformational rearrangement from free to bound TAR [56]. Reyes et. al have investigated the differences in previously studied structures and trajectories, particularly in the formation of the U-A-U base triple, the dynamic flexibility of the Tat peptide, and the interactions at the binding interface. They have also calculated the relative binding of different Tat peptide mutants to TAR RNA and found qualitative agreement with experimental studies. The molecular dynamics simulations show that the starting structures in which KkN binds to the major groove of TAR (as it is the case for the Tat-TAR complex of HIV-1) are unstable [53]. Molecular dynamics simulation studies along with docking suggest that several attractive interactions between the native Tat (1-9) and dipeptidyl peptidase IV lead to a stable complex and that the reduced affinity of both L6-Tat (1-9) and I5-Tat (1-9) derivatives

might be caused by conformational alterations in comparison to the parent peptide [103]. In an attempt to shed light on the molecular basis of the functional differences found for Tat mutants a series of molecular dynamics simulations have performed on modified Tat proteins from HIV-1 strain Z2. Remarkable correlation is found between the degree of structure conservation and the transactivation capabilities of Tat mutants [104]. The studies illustrate the relation between structural dynamics of the protein and its residues with its function and activation. The nature of the dynamics is varied according to the residue position, sequence and structure.

2.7. Molecular Phylogenetics

Mutation takes place in genome of every organism. The single nucleotide shift is due to the insertion or deletion of the nucleotides. These mutations are randomly caused by error in the replication machinery and are essential for the natural selection process. By comparing the sequence of the genome (DNA) or the functional elements (RNA, protein) of different isolates or species conclusion about the evolutionary relationship, functional and structural variations can be drawn [57].

Molecular phylogenetic analysis detects evolutionary relationships among organisms. Phylogenetic trees can represent these relationships. A phylogenetic tree is a graph consisting of nodes and branches where only one branch connects any two adjacent nodes. The nodes represent the taxonomic unit. The algorithms use sequences of DNA, RNA or protein to construct the trees. These sequences are first prepared, shorted and aligned. The quality of these alignments affects the reliability of the tree.

The most commonly used methods to construct phylogenies include parsimony, maximum likelihood, and MCMC-based Bayesian inference [58]. Distance-based methods construct trees based on overall similarity which is often assumed to approximate phylogenetic relationships. All methods depend upon a mathematical model describing the evolution of characters observed in the species included. They are usually used for molecular phylogeny where the characters are aligned nucleotide or amino acid sequences. The use of phylogenetics in viral studies has increased dramatically in the last years. When estimating phylogenetic relationships among DNA sequences, the use of a model of nucleotide substitution is necessary. While maximum parsimony assumes a model of evolution in an implicit manner taking the number of mutation required to convert one sequence to another, distance methods and maximum likelihood explicitly

estimate parameters according to the model of evolution specified [59, 60]. Distance methods estimate only the substitution rate, while maximum likelihood estimates all the parameters of the model. Many viral evolutionary studies have focused on the HIV-1 virus. Likewise, many genes show a bias in transitions over transversions, again affecting the rate of change from one nucleotide to another.

An important factor that affects the accuracy of tree reconstruction is whether the data analyzed actually contain useful phylogenetic signal, a term that is used generally to denote whether related organisms tend to resemble each other with respect to their genetic material or phenotypic traits [61, 62].

2.8. Structural Prediction

The experimental methods used for determining structure, including NMR and X-ray crystallography, are time consuming and can depend on initial secondary structure models for developing constructs. The structure can also be predicted computationally by inter relating various physical, chemical and mathematical rules, and considering various factors. Mathematical models and algorithms are needed for incorporating those rules into a physical structure. Parameters those define the structure have to be selected for creating these rules [63]. The methods devised for predicting the structure are comparative or homology modeling and ab initio method with computer algorithm. Comparative protein modelling uses previously solved structures as starting points, or templates. Ab initio- or de novo- protein modelling methods seek to build three-dimensional protein models based on physical principles rather than on previously solved structures. Structure is usually determined by the comparative analysis of multiple homologous sequences. When homologous sequences are not available, free energy minimization by dynamic programming can be used to predict the structure of a single sequence [64]. Till now homology modeling gives more accurate protein structures than any other method.

2.8.1. Homology modeling

Comparative or homology modeling uses experimentally determined protein structures to predict the conformation of other proteins with similar amino acid sequences. Small changes in the sequences is accordingly reflected in the structure. Till now homology modeling remains most accurate method to predict the protein structure [65]. Although several procedures exist in the public domain, the choice of the right

method is not unambiguous. Study shows that Modeller gave best results amongst the chosen protocols [66]. Modeler produces protein homology models, given a template and sequence alignment. The structures are predicted based on distance restraints obtained from the template, from the database of crystal structures in the PDB, and from a molecular force field. Ligand structures and constraints such as disulfide bonds and cis-prolines can be incorporated into the model building step. Loops are generated de novo, by a process that incorporates knowledge-based potentials from known crystal structures [67]. Homology modeling consists of building a protein model using a structural template, the template being a protein of known structure. The basic outline of the procedure is shown in Figure 5. The sequences of the two proteins, the target (or unknown) protein and the template, are first aligned. The Cα coordinates of the aligned residues from the template are then copied over to the target to form the skeletal backbone. The residue side chains, and relative insertions and deletions, are then modeled using automated or semi-automated procedures. Finally, the protein model thusly obtained may be subjected to energy minimization or molecular dynamics to relax unfavorable contacts. The quality of the sequence alignment is critical in determining model quality [68]. The quality of the homology model is dependent on the quality of the sequence alignment and template structure. The approach can be complicated by the presence of alignment gaps (commonly called indels) that indicate a structural region present in the target but not in the template, and by structure gaps in the template that arise from poor resolution in the experimental procedure (usually X-ray crystallography) used to solve the structure. Model quality declines with decreasing sequence identity; a typical model has ~2 Å agreement between the matched C_α atoms at 70% sequence identity but only 4-5 Å agreement at 25% sequence identity. Regions of the model that were constructed without a template, usually by loop modeling, are generally much less accurate than the rest of the model, particularly if the loop is long. Errors in side chain packing and position also increase with decreasing identity, and variations in these packing configurations have been suggested as a major reason for poor model quality at low identity [69].

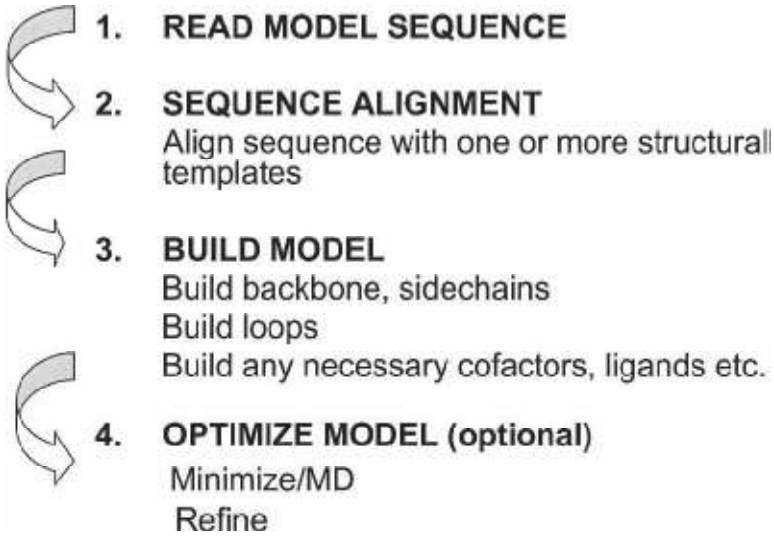

Figure-5: Outline of steps for homology modeling process.

Molecular dynamics simulation

Molecular dynamics (MD) is a form of computer simulation in which atoms and molecules are allowed to interact for a period of time under known laws of physics, giving a view of the motion of the atoms. Molecular dynamics probes the relationship between molecular structure, movement and function [70]. Molecular dynamics is a specialized discipline of molecular modeling and computer simulation based on statistical mechanics Computational methods have been used in biology for sequence analysis, all-atom simulation, and more recently for modeling biological networks. Of these three techniques, all-atom simulation is currently the most computationally demanding, in terms of compute load, communication speed, and memory load [71]. The molecular dynamics method was first introduced by Alder and Wainwright in the late 1950's [70] to study the interactions of hard spheres. Many important insights concerning the behavior of simple liquids emerged from their studies.

Molecular dynamics simulations generate information at the microscopic level, including atomic positions and velocities. Statistical mechanics is required for the conversion of this microscopic information to macroscopic observables such as pressure, energy, heat capacities, etc. Statistical mechanics is fundamental to the study of biological systems by molecular dynamics simulation. In a molecular dynamics simulation, the macroscopic properties of a system is explored through microscopic simulations, for example, to calculate changes in the binding free energy of a particular ligand, or to examine the energetics and mechanisms of conformational change. The

connection between microscopic simulations and macroscopic properties is made via statistical mechanics which provides the rigorous mathematical expressions that relate macroscopic properties to the distribution and motion of the atoms and molecules of the N-body system. Molecular dynamics simulations provide the means to solve the equation of motion of the particles and evaluate these mathematical formulas. With molecular dynamics simulations, one can study both thermodynamic properties and/or time dependent (kinetic) phenomenon [72, 73, 74].

In molecular dynamic simulations the atoms of a system move according to the Newtonian equations of motion

$$F_i = m_i a_i$$

Where F_i is the force exerted on particle i, m_i is the mass of particle i and a_i is the acceleration of particle i. The force can also be expressed as the gradient of the potential energy,

$$F_i = -\nabla U_t$$

Combining these two equations yields

$$\frac{dU_{total}}{dr_i} = m_i \frac{d^2 r_i}{dt^2}$$

Where U_{total} is the potential energy of the system. Newton's equation of motion can then relate the derivative of the potential energy to the changes in position as a function of time.

Highly simplified description of the molecular dynamics simulation algorithm is given in figure-6 [75]. The simulation proceeds iteratively by alternatively calculating forces and solving the equations of motion based on the accelerations obtained from the new forces. In practise, almost all MD codes use much more complicated versions of the algorithm, including two steps (predictor and corrector) in solving the equations of motion and many additional steps for e.g. temperature and pressure control, analysis and output.

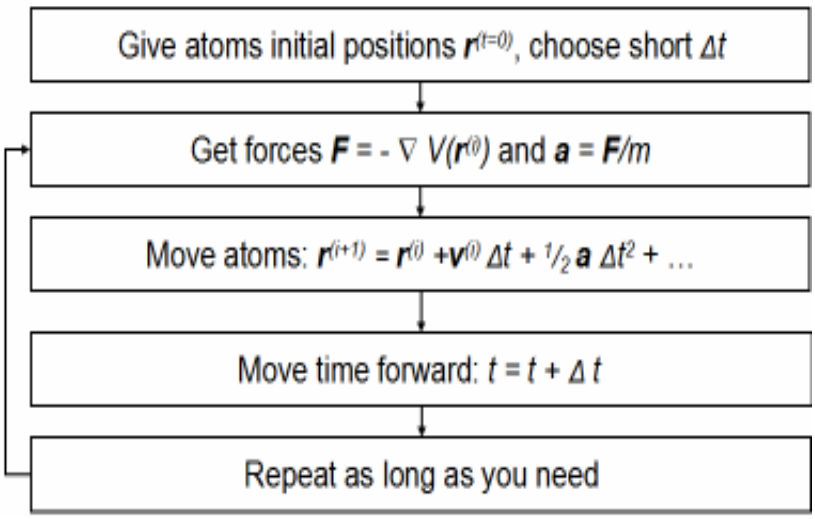

Figure-6: Molecular dynamics simulation algorithm [75]

2.9.1. Force Field Functions

The potential energy, represented through the MD "force field," is the most crucial part of the simulation because it must faithfully represent the interaction between atoms, yet be cast in the form of a simple mathematical function that can be calculated quickly. For an all-atom MD simulation, one assumes that every atom experiences a force specified by a model force field accounting for the interaction of that atom with the rest of the system. Today, such force fields present a good compromise between accuracy and computational efficiency. NAMD employs a common potential energy function that has the following contributions [105]:

$$U_{total} = U_{bond} + U_{angle} + U_{dihedral} + U_{vdW} + U_{coulomb}$$

Where bonds counts each covalent bond in the system, angles are the angles between each pair of covalent bonds sharing a single atom at the vertex, and dihedral describes atom pairs separated by exactly three covalent bonds with the central bond subject to the torsion angle Ø (Fig. 7). An "improper" dihedral term governing the geometry of four planar, covalently bonded atoms is also included as depicted in Figure-7. The final two terms in equation describe interactions between nonbonded atom pairs, which correspond to the van der Waal's forces (approximated by a Lennard–Jones potential) and electrostatic interactions, respectively.

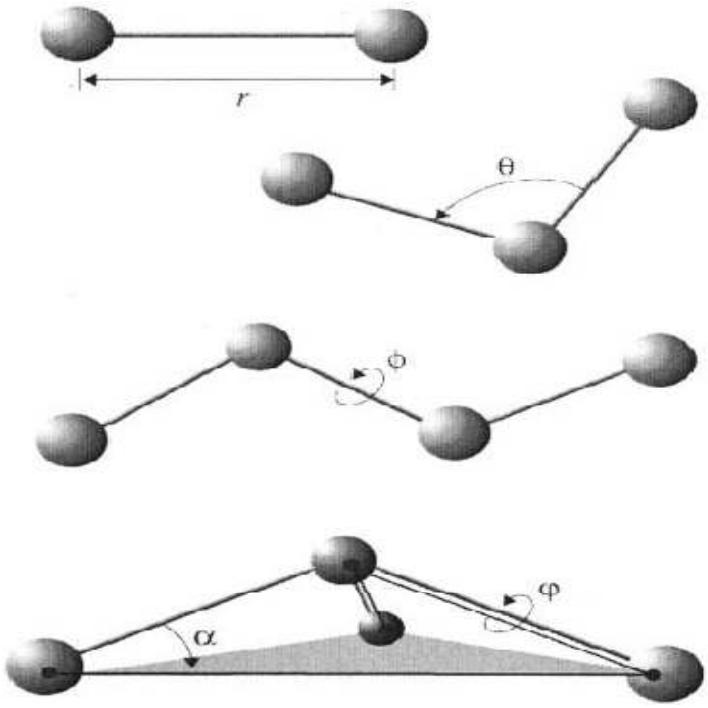

Figure-7: Internal coordinates for bonded interactions: r governs bond stretching; θ represents the bond angle term; Ø gives the dihedral angle; the small out-of-plane angle α is governed by the so-called "improper" dihedral angle φ [105].

To avoid surface effects at the boundary of the simulated system, periodic boundary conditions are often used in MD simulations. The particles are enclosed in a cell that is replicated to infinity by periodic translations. A particle that leaves the cell on one side is replaced by a copy entering the cell on the opposite side, and each particle is subject to the potential from all other particles in the system including images in the surrounding cells, thus entirely eliminating surface effects. Because every cell is an identical copy of all the others, all the image particles move together and need only be represented once inside the molecular dynamics code. However, because the van der Waals and electrostatic interactions exist between every nonbonded pair of atoms in the system (including those in neighboring cells) computing the long-range interaction exactly is unfeasible. To perform this computation, the van der Waals interaction is spatially truncated at a user-specified cutoff distance. For a simulation using periodic boundary conditions, the system periodicity is exploited to compute the full (nontruncated) electrostatic interaction with minimal additional cost using the particle-mesh Ewald (PME) method described in the next section.

2.9.2. Full Electrostatic Computation

Ewald summation is a description of the long-range electrostatic interactions for a spatially limited system with periodic boundary conditions [106]. The infinite sum of charge-charge interactions for a charge-neutral system is conditionally convergent, meaning that the result of the summation depends on the order in which it is taken. Ewald summation specifies the order as follows: sum over each box first, then sum over spheres of boxes of increasingly larger radii. Ewald summation is considered more reliable than a cutoff scheme, although it is noted that the artificial periodicity can lead to bias in free energy, and can artificially stabilize a protein that should have unfolded quickly. Dropping the prefactor $1/4\pi\varepsilon$, the Ewald sum involves the following terms:

$$E_{\text{Ewald}} = E_{\text{direct}} + E_{\text{reciprocal}} + E_{\text{self}} + E_{\text{surface}}$$

The particle–mesh Ewald (PME) method is a fast numerical method to compute the Ewald sum [86]. The PME method does not conserve energy and momentum simultaneously, but neither does the particle-particle/particle-mesh method or the multilevel summation method. Momentum conservation can be enforced by subtracting the net force from the reciprocal sum computation, albeit at the cost of a small long-time energy drift.

2.9.3. Numerical Integration

Biomolecular simulations often require millions of time steps. Furthermore, biological systems are chaotic; trajectories starting from slightly different initial conditions diverge exponentially fast and after a few picoseconds are completely uncorrelated. However, highly accurate trajectories are not normally a goal for biomolecular simulations; more important is a proper sampling of phase space. Therefore, for constant energy (NVE ensemble) simulations, the key features of an integrator are not only how accurate it is locally, but also how efficient it is, and how well it preserves the fundamental dynamical properties, such as energy, momentum, time-reversibility.

Designing drugs or vaccine against Human immunodeficiency virus has been facing failure due to the variability of the structural motifs against which the drugs are being designed. Motif with constant structural features across strains, time and geographical regions will be a very good target for which stable drugs or vaccines can be designed. Phyllogenetic analysis will be helpful in finding such structures across diversities. In

comparison to structural genes and proteins like env and gag, regulatory protein (tat, rev) and structural elements like TAR, RRE show more constancy in sequence and structure. Targeting RNA has some advantages as compared with targeting proteins. More sites are accessible at the RNA level; whereas the active site of a protein is often the only target. Proteins that share a common substrate like ATP or ligands are difficult to inhibit specifically. It is possible to develop multivalent drugs to target RNA or drugs that target a RNA sequence that is essential for encoding an important sequence of a protein. RNA elements TAR and RRE also have very conserve structural features which are effective binding site for tat and rev protein respectively. The binding of these two proteins to their respective elements is very crucial for replication and assembly of virus. Study of structure and binding properties with molecular dynamics simulation methods will help in designing strategies for inhibition of the virus spreading and migration.

Chapter 3

3. **Methods**

3.1. Sequence and alignment

The nucleotide and peptide sequences of the thirty two isolates described here are available under EMBL accession numbers. The sequences of the Tat protein are collected from Rfam database (http://www.sanger.ac.uk/cgi-bin/Rfam/) [76]. All sequences are manually checked for anomalies using Bioedit program. Residues from position 1 to 86 of the protein segment are only taken for alignment. Sequence variability is considered while choosing the sequences. The sequences are selected from different geographical regions and subgroups. A selective random approach was taken while deciding a sequence from the database. The description of the sequences are given in table-1.

The selected HIV and SIV tat sequences were aligned using ClustalW with reference to Blossom-62 substitution matrix (http://www.ebi.ac.uk/clustalw) [77]. Distances between pairs of sequences were estimated using the Protdist program of the Phylip package provided by Dr J. Felsenstein. Consensus sequence was generated from the aligned sequences using cons program of Emboss package [78].

Residue wise comparison of the consensus sequence with the aligned sequences was carried out by Bioedit. Assignment of residues at each position was determined by comparing the residue frequency at the position in the aligned sequences and with that of structures available at protein data bank. Three sequences were generated on the basis of sequence based variation from the consensus sequence. The distance between the sequences are compared with Protdist provided in the Phylip package with reference to PAM matrix.

Table-I Description of the sequences considered for checking the variance.

No.	Accession No.	Description
1	AF004885.1	HIV-1 isolate Q23-17 from Kenya, complete genome.
2	AF005494.1	HIV-1 isolate 93br020 from Brazil complete genome.
3	AF033819.3	HIV-1, complete genome
4	AF042100.1	HIV-1 isolate MBC200 from Australia, complete genome.
5	AF049337.1	HIV-1 clone 94CY032-3 from Cyprus, complete genome.
6	AF061640.1	HIV-1 isolate HH8793 clone 1.1 from Finland, complete genome.
7	AF063223.1	HIV-1 isolate DJ263 from Djibouti, complete genome.
8	AF064699.1	HIV-1 isolate BFP90 from Burkina Faso, complete genome.
9	AF067154.1	HIV-1 isolate 301999 from India, complete genome.
10	AF069140.1	HIV-1 isolate DH12 clone 3 from the USA, complete genome.
11	AF069671.1	HIV-1 isolate SE7535 from Uganda, complete genome.
12	AF070521.1	HIV-1 E9 from the USA, complete genome.
13	AF076474.1	HIV-1 isolate VI354 from Gabon, complete genome.
14	AF084936.1	HIV-1 subtype G, Democratic Republic of the Congo, complete genome
15	AF086817.1	HIV-1 strain LM49 isolate TWCYS from Taiwan, complete genome.
16	AF115393.1	Simian immunodeficiency virus strain SIVcpz, complete genome.
17	AF164485.1	HIV-1 isolate 93TH902.1 from Thailand, complete genome.
18	AF179368.1	HIV-1 strain GR17 from Greece complete genome.
19	AF193277.1	HIV-1 isolate RU98001 from Russia, complete genome.
20	AF197340.1	HIV-1 isolate 90CF11697, Central African Republic, complete genome
21	AF224507.1	HIV-1 strain HIV-1wk from Korea, complete genome.
22	AF256205.1	HIV-1 clone S61D15 from Spain, complete genome.
23	AF286225.1	HIV-1 strain 96ZM751 from Zambia, complete genome.
24	AF286226.1	HIV-1 strain 97CN001 from China, complete genome.
25	AF286227.1	HIV-1 strain 97ZA012 from South Africa, complete genome.
26	AF286233.1	HIV-1 strain 98IS002 from Israel, complete genome.
27	AF290028.1	HIV-1 clone C.96BW06.J4 from Botswana, complete genome.
28	AF332867.1	HIV-1 isolate A027 from Argentina, complete genome.
29	AF385934.1	HIV-1 isolate URTR23 from Uruguay, complete genome.
30	AF413987.1	HIV-1 isolate 98UA0116 from Ukraine, complete genome.
31	AF465242.1	Simian-Human immunodeficiency virus isolates 1B3, complete genome.
32	AY586540.1	HIV-1 isolate CU76 from Cuba, complete genome.

3.2. Homology modeling and structure analysis

The protein structure databases were searched for the protein consensus sequence using BLAST and PSI-BLAST. Initial sequential similarity of each modified consensus sequence with sequence of the structures was carried out by ClustalX. Residue-by-residue geometry and overall structure geometry was analyzed for checking stereo chemical quality of downloaded protein data bank structures by Procheck [79]. Protein template for homology modeling was selected considering the overall structural quality and sequential and structural similarity with the consensus sequences. Blast [80] search among the proteins of known 3D structure revealed that the three structures from protein data base 1tac, 1tbc and 1tiv showed the considerable sequence identity score with our sequences. Out of these structures 1tac misses crucial cystein residues and 1tiv scores very less in stereo chemical quality. Hence, in this study NMR structure of Tat (PDB code: 1tbc) [47] was selected as a template and based on this structure the 3D consensus structures were predicted.

The alignment of the sequences with the template structure was done using Bodil [81]. The structures were generated from the sequence alignment and the structural template using the Modeler program (http://salilab.org/modeller) [82]. The computed structure of the Tat obtained was refined by energy minimization with NAMD 2.5 (http://www.ks.uiuc.edu/Research/namd) [83] for 10 ps with restraint on the backbone of the protein taking CHARMM force field until the energy showed stability in sequential repetition.

The conformational stability of the so predicted theoretical model was evaluated sterically with Procheck [79]. The modeled structures are visualized and structurally by Chimera [84]. The hydrogen interactions are predicted with constraint 0.4A and angle 20 degree.

3.3. Molecular dynamics simulation

Molecular dynamics simulations of the modeled proteins are were performed using NAMD 2.5. The protein was immersed in a rectangular box of TIP3P waters [85] providing a 5 Å buffer from the protein to the periodic boundary in each direction. The bonded interactions were calculated at every time-step, the short-range nonbonded interactions at every two time-steps, and the long-range electrostatics interactions at every four time-steps. The pair-list of the non-bonded interaction was recalculated every

20 time-steps with a pair-list distance of 13.5 Å. The short-range non-bonded interactions were defined as Van der Waals and electrostatics interactions between particles within 12 Å. A smoothing function was employed for the Van der Waals interactions at a distance of 10Å. The long range electrostatic forces were calculated with the particle-mesh Ewald [86]. CHARMM27 [87] force-field parameters were used in all simulations in this study. Periodic boundary conditions and water wrapping were activated in the simulations. The SHAKE routine with a tolerance of 10^{-8} Å was used in all simulations. In order to remove spurious contacts, a set of 13,000 energy minimization steps were carried out. The first 3,000 steps were performed taking the protein backbone was fixed, minimizing all other atoms. No constraints were applied during the last 10,000 steps, freely minimizing all atoms.

The system was simulated for with 1 atm constant pressure and 310K constant temperature (NPT) [88] using the Nose´-Hoover Langevin piston pressure control [89] and the Langevin damping dynamics [90] respectively. In next 400 ps the restraint on the protein backbone is removed completely in a stepwise manner. Then the system in is simulated without any restraint for 1600 ps continuously. So a simulation of 2 ns is achieved. The atomic coordinates and velocities were saved every 500 time-steps, and coordinate trajectories were saved every 250 time-steps for subsequent data analysis. It took approximately two day to achieve 1 ns simulation for the system using eight 1.15-GHz EV7 processors on the HP micro tower.

Chapter 4

4. Results and Discussion

4.1. Sequence divergence

The alignment shows the sequence variability of the tat protein across the geographical distribution. The phylogenetic tree in figure is showing three branches on the basis of amino acid sequence similarity. The first branch consists up of sequences from Brazil, Uruguay, and Argentina. In the second branch sequences from countries Taiwan, Australia, Spain, USA, Russia, and Korea are segregated. All other sequences are grouped under the third branch. The sequence from the cpzsiv can be clearly seen as an out group. The consensus structures conceived in the study more or less represent each of these groups.

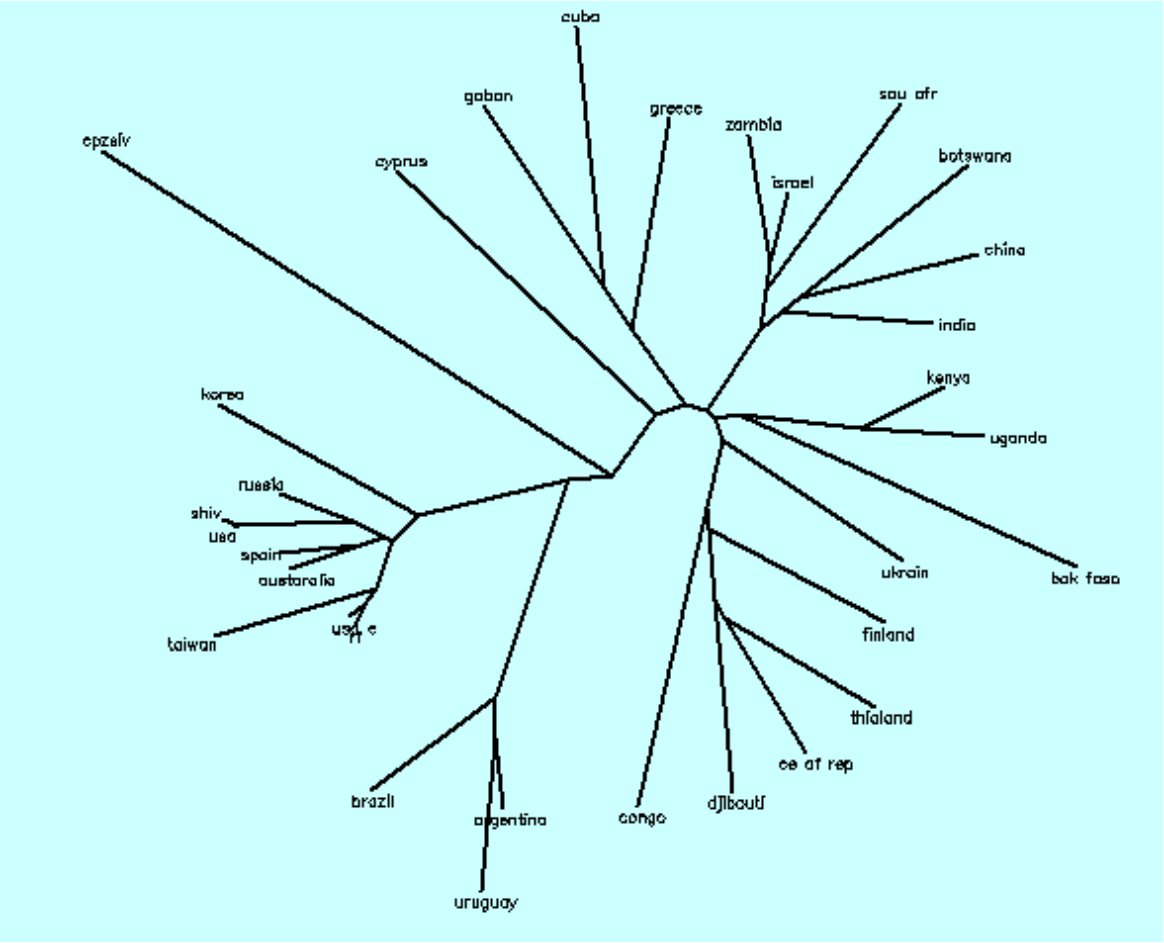

Figure-8: Constructed phylogeny of the Tat data showing geographical variation.

The section wise variation of the residues in the protein sequences is shown in the table-II. Residues from position 1 to position 40 are moderately conserved with most of

the positions are highly conserved and some are partially conserved with strong or weak groups for substitution. The cystein residues are highly conserved as they are part of structurally important sulphur bonds. The core region (aa 38–48), which is highly conserved among other lentiviruses also shows high degree of conservancy.

Table-II: Conservancy of amino acid positions across the sequences. Partially conserved groups are all the positively scoring groups that occur in the Gonnet Pam250 matrix. The strong and weak groups are defined as strong score >0.5 and weak score =<0.5 respectively.

Sequence	Conserved	Partially Conserved		Sequence	Conserved	Partially Conserved	
		Strong gr.	Weak gr.			Strong gr.	Weak gr.
1-10	1,5,6,8,10	2,4,9	-	51-60	51-3,55, 56	-	-
11-20	11,14-5, 18,20	13,17	16	61-70	-	66	65
21-30	21,25,27. 28,30	26	23	71-80	72	72,79	-
31-40	33,34,37, 38	-	40	81-86	-	82,85,86	83,84
41-50	41,42-50	-	43				

The basic ARD region (aa 48-56) contains the nuclear localization signal of the protein [91] and specifically interacts with a uridine-rich bulge motif in the RNA TAR [48]. So, it shows high conservancy for maintaining functional viability of the protein. The core region, which has been proposed to provide structural stabilization to the protein [92] is least conserved. The structural stability, which is mostly dependent on residual interactions, is maintained in expense of the residual substitution and in favor of stronger interaction. The residues from 81 to 86 are moderately conserved.

Three consensus sequences are formed based on the position specific variability of the residues. The positional variations of the residues among the models are shown in table-III. As expected the variations are mainly concentrated at first and last sections of

the sequences. Out of 13 positional variations studied, the first eight (aa 3-35) show residual substitution within strong groups (Table-II). These positions are inside the region important for maintaining the functional viability of the protein. Any distant substitution with unrelated amino acid may disrupt the activity. The distance between the sequences is shown in the table IV. The sequence SA and C are maximum apart where as sequence SA and B are least apart. As the SA is modeled on the sequences from South America and the model B chiefly represents the sequences from Europe and North America the similarities are justified.

Table-III: Variation of amino acid positions across the modeled structures.

Models	positions												
	3	7	12	19	21	23	24	35	61	64	67	68	77
SA	L	N	N	T	P	T	R	Y	N	T	V	S	T
B	P	N	N	K	A	T	N	Q	N	T	V	S	P
C	P	R	K	K	A	N	K	Q	S	D	N	P	T

Table-IV: Distance between the modeled sequences calculated by Protdist.

	Distance		
Models	SA	B	C
SA	0	0.0914	0.184
B	0.0914	0	0.125
C	0.184	0.125	0

4.2. Structural variability

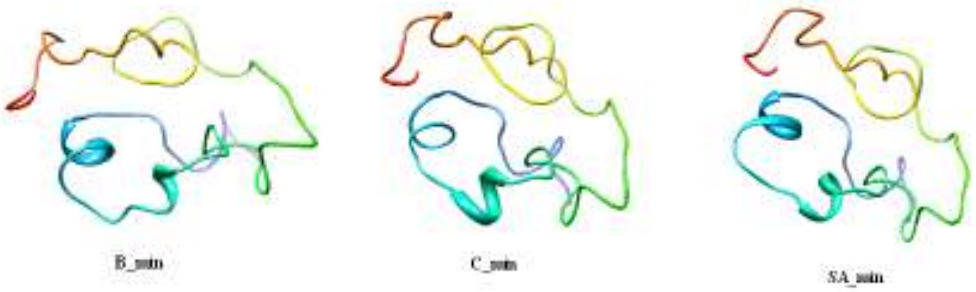

Figure-9: The Tat consensus structures from 32 protein sequences (Table-I) modeled on PDB: 1tbc. The helix 1 (blue) and helix 2 (green) are clearly visualized.

The structures though modeled on same template show structural variability. Although Tat does not present secondary structure elements [54], the models after minimization show the two helical regions (Figure-9). The first helix forms in between positions 16S to 20T (Figure-10). In model B the helix is stabilize by the hydrogen interaction between 16S and 20T. Extra-helical hydrogen interactions are in between 14P and 82T, 16S and 82T, 21A and 23T, 19K and 25C. Though a helical structure is formed between 15G to 21A the helix is not distinct in model C. In the helical structure there is a hydrogen interaction between 16S and 20T, 16S and 21A. Extra-helical hydrogen interactions are in between 16S and 82T, 14P and 82T, 20T and 23N, 19K and 28K. Lysine at position 19 forms a hydrogen interaction with 64D. Availability of lysine at this position is the distinctive feature of C model and may be responsible for the splintering of helix. In model SA the helix is stabilize by the hydrogen interactions between 15G and 19T, 16S and 20T. Extra-helical hydrogen interactions are in between 14P and 82T, 16S and 82T, 18P and 23T. The residues at position 23, 25, 64, 84 are important for maintenance of helix structure.

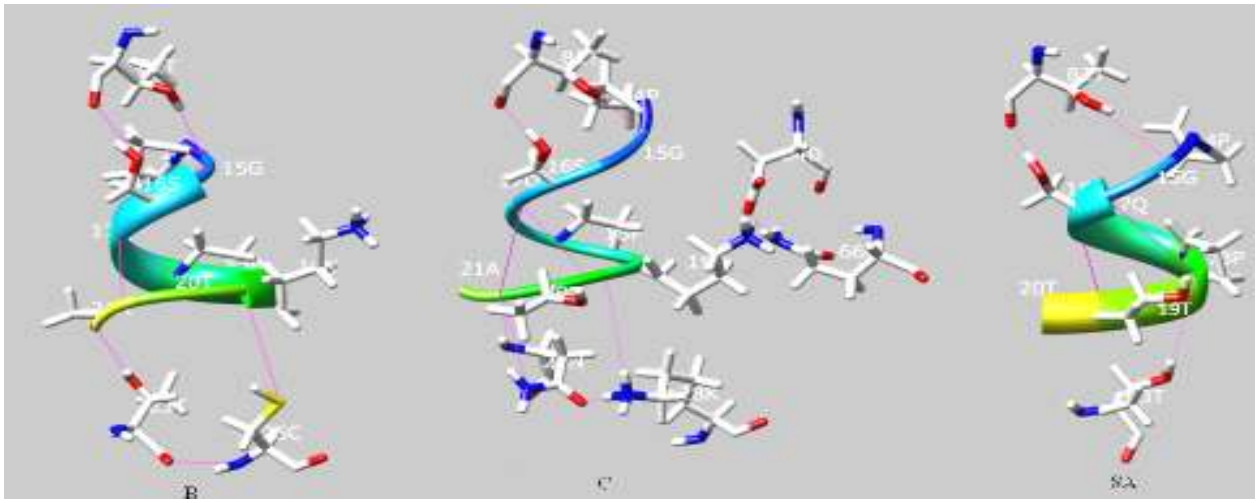

Figure-10: A view of the first helix (residue ~16-20) of the consensus structures and their hydrogen interactions (pink lines) with other neighboring residues.

The second characteristic helix positions itself in between 25 to 29 amino acids (Figure-11). In model B the helix consists of amino acid of 27 to 29 positions. Secondary structure prediction also confirms formation of helix in this region (unpublished data). The helix is stabilized by the hydrogen interaction between 27C and 30C. There are hydrogen interactions between 27C and 32Y, 30C and 32Y, 28K and 25C, 29K and 25C. This shows the role of 25C and 32Y in stabilization of the helix. In model C a distinct

and well defined helix is formed though the residues 25 to 29. Intra helix hydrogen interactions can be seen between 24K and 28K, 25C and 29K, 26Y and 30C. Other hydrogen interactions are in between 23N and 19K, 28K and 19K. The lower part of the helix is forming hydrogen interactions as 28K and 32Y, 30C and 32Y. In model SA the helix consists of 26 to 29 residues. The helix is stabilized by the hydrogen interaction between 25C and 29K, 26Y and 30C. There is a hydrogen interaction in between 24R and 26Y is essential for formation of helix.

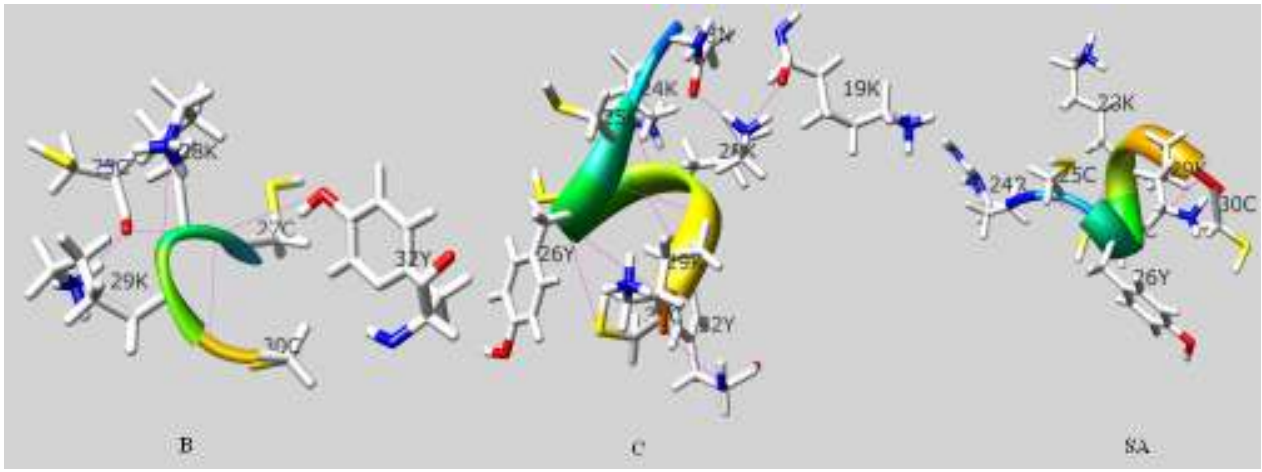

Figure-11: The view of second helix (residue ~ 26-30) of the consensus structures and their hydrogen interactions (pink lines) with other neighboring residues.

Churcher et al. have demonstrated the importance of sequence from position 48G to 59P in recognition and attachment to the TAR RNA element [93]. The arrangement of these residues and their hydrogen interaction formation with the neighboring residues can be visualize by table-V. The motif is stabilized by hydrogen interactions with some of the distant residues like 2E, 5D, 9E, 35Q, 44G. The glutamine residue at position 54 which takes a crucial role in binding to TAR RNA element shows highest number of hydrogen interactions. The arginine rich central part aa (52-57) also shows higher number of hydrogen interactions. The interaction between the basic region and the glutamic acid residue at position 2 as described by Pantano et al. can be clearly visualized [54].

Table-V: Hydrogen interactions formed in the RNA binding motif (48-59) across the models. The interaction (H.B) is shown between the residues (res.) among the models.

B		C		SA	
Res.	H.B	Res.	H.B	Res.	H.B
48G		48G		48G	50K
49R	44G(2), 33H(2)	49R	44G, 32Y,67N	49R	44G(2)
50K	52R, 2E	50K	52R	50K	48G, 2E
51K		51K	53R, 54Q(2)	51K	
52R	50K,54Q,55R	52R	50K	52R	54Q, 55R
53R	54Q, 35Q	53R	51K, 35Q	53R	54Q
54Q	52R, 53R,57R	54Q	51K, 56R	54Q	52R,53R, 56R
55R	5D	55R	5D	55R	52R, 5D
56R	9E	56R	54Q, 9E, 63Q	56R	54Q, 9E
57R	54Q	57R	60Q	57R	68S
58T		58T		58T	
59P		59P	63Q	59P	65H

4.3. Dynamics of residue patches and active pockets

Three molecular dynamics simulations of two nanosecond each were carried out on the models in order to investigate their stability and dynamical properties. Each systems were simulated without constraints and reached equilibrium after approximately 1.2 ns of constant pressure and temperature equilibration at 1 atm and 310 K. Correspondingly, the trajectory time from 0–1.2 ns is referred to as the "equilibration phase" and from 1.2–2 ns is referred to as the ''dynamics phase'' (Figure-12). Plots of the time evolution of the root mean square deviation (RMSD), where each trajectory frame was aligned to the initial starting structure in order to remove any rotational or translational motion, indicate that equilibration was achieved for all systems. The overall root-mean-square-fluctuations (RMSF) per residue was calculated during the dynamics phase for each system based on Cα positions after alignment to the average equilibrated structure, and the resulting RMSF difference plot shows the differences in RMS fluctuations between the three systems (Figure-13). The average RMSFs of the residues of models B, C and SA is 2.18, 1.16 and 1.48 respectively.

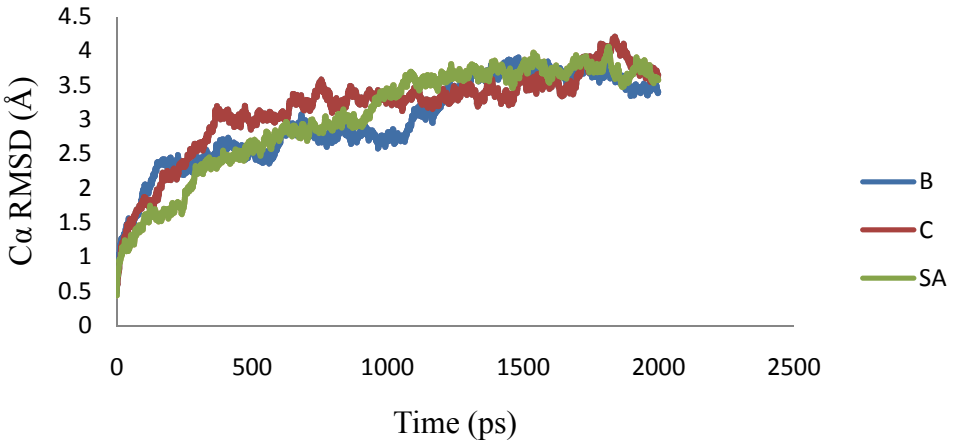

Figure-12: Root mean square deviation (RMSD) of the models plotted as a function of simulation time of 2 ns.

Position of the residue and its interaction with other residues defines the structure of the protein and also characterize its molecular dynamics motion. Residues adjacent to glycine and proline show marked motion due to their conformational flexibility. The presence of 5'GLGI3' motif in between position 42 to 45 explains the increased fluctuation of this region (Figure-13). The role of this region as a hinge between the trans-activating core region and RNA binding ARD can be reasoned for this dynamics. The location of polar uncharged amino acid aspargine at position 24 in model B instead of a basic amino acid lysine and arginine as in model C and SA is responsible for increased fluctuation of the residues near to the said position.

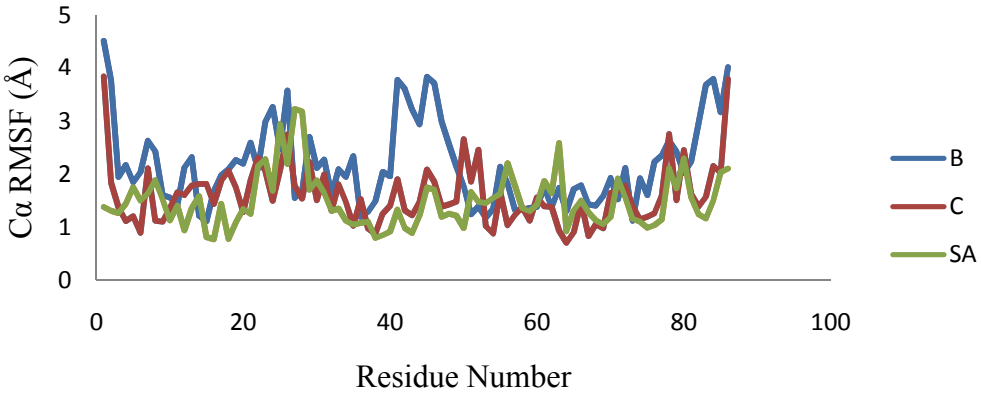

Figure-13: Structural flexibility shown as RMSFs of all Cα atoms of the models from the last 800 ps of unrestrained simulations.

The residues from 48G to 59P consisting the RNA binding arginine rich domain (ARD) are showing least motion as compared to other residues (Figure-14b). This pocket

as a motif is stabilized by various hydrogen interactions with neighbor residues (Table-V). The arginine at 52 in model C shows increased motion due to lesser number of hydrogen interactions as compared to other structures. The exact opposite can be applied for arginine at position 56 as it shows less motion in model C as compared to other models. Glutamine at position 53, a very important residue in binding to TAR RNA shows less motion as it is well stabilized by hydrogen interactions with other residues. The residues 2E, 5D, 9E, 33H, 44G which are important for maintaining the RNA binding pocket (Table-V) are showing reduced motion as compared to other residues. This is to conserve the structure of the protein for functional viability.

Table-VI: Comparisons of residual variations (RMSFs) of Cα atoms of the models at selected positions (Table-III) from the last 800 ps of unrestrained simulations.

Res.No.	Models					
	SA		B		C	
3	L	1.949309	P	1.375736	P	1.263088
7	N	2.631948	N	2.312005	R	1.634231
12	N	2.123034	N	1.804578	K	0.939108
19	T	2.269854	K	1.74876	K	1.092498
21	P	2.59306	A	1.891883	A	1.247441
23	T	2.987654	T	2.055694	N	2.280313
24	R	3.272842	N	1.498669	K	1.679775
35	Y	2.340913	Q	1.024713	Q	1.050018
61	N	1.746667	N	1.392315	S	1.869763
64	T	1.303023	T	0.705819	D	0.923727
67	V	1.432402	V	0.835493	N	1.279583
68	S	1.407785	S	1.05363	P	1.123748
77	T	2.350838	P	1.603655	T	1.144498

Considering the taken residual variations among the models (Table-III) the RMSFs of residues at each position across the models are given in Table-VI. The RMSFs for the similar residues among the models at a position are almost equal in the NT and CRT region (positions in between 3 to 35). But it is not true for residues in QRD and CT where the interactions rather than nature of the nature of the residue are vital for

maintaining the stability of the protein. In these regions the models though contain similar residues show dissimilar RSMFs and vice versa.

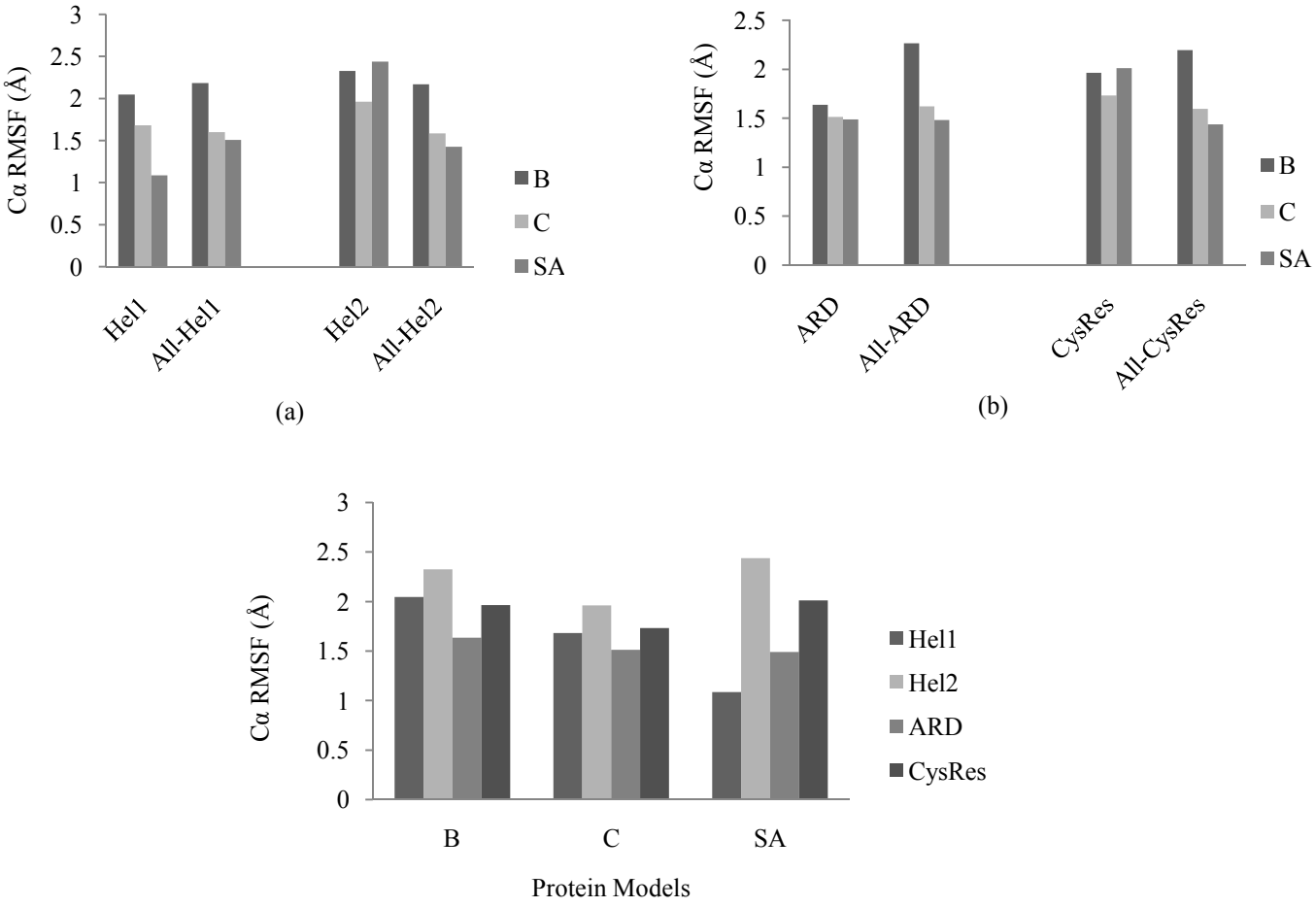

Figure-14: Variation in average fluctuation (RSMF) of Cα atoms of residues constituting (a) helical domains (b) Arginine Rich Domain (ARD), cystein residues and (c) all structural domains of Tat protein across the models from the last 800 ps of unrestrained simulations. Hel1: Helix1 (residue16-20), Hel2: Helix2 (residue26-30), ARD: Arginine Rich Domain (residue48-59), CysRes: Cystein Residues, All-Hel1, All-Hel2, All-ARD, All-CysRes: All other residues except those of respective structural domains.

The QRD which has been proposed to provide structural stabilization to the protein [92], is showing almost homogeneous variation though out the models (Figure-13). The reverse is true for the cysteine-rich domain (aa 22–37) and the core region (aa 38–48) rich in hydrophobic residues this region is crucial for Tat trans-activation [48, 92] which have a varying RMSF for the residues (Figure-14b). Though the domains have a

varied motion with a diverse average RMSF in a protein structure, they maintain a specific homogeneity when compared across the models. The second helix in the core region always shows the highest RMSF where as the ARD shows the lowest (Figure-14c) though out the models. Similarly the model B shows highest and model SA shows the lowest deviation when the domains are considered (Figure-14a, b).

The helix 1 which comprises of roughly residue 16S to residue 19 shows minimal motion across the models with average RMSF of 1.085 in SA, 2.045 in B and 1.685 in C (Figure-14c). Notably, the helix-1 exhibits marked stability with lower RMSF (Figure-14a) as compared to rest of the residues. There is an increased RMSD after disruption of the helix from position 21. In model C where the helix-2 is not well defined the residues have an increased RMSF of 2.43 compared to other models at those positions. The residues of helix2 which are positioned roughly from 26 to 29 have an increased motion as compared to helix 1 due to its undefined nature except model C. In model C where it has a very stable conformation the residues have a lower average RMSF of 1.9 compared to other models. The position of this structure in the catalytically dynamic core region also explains the increased fluctuation.

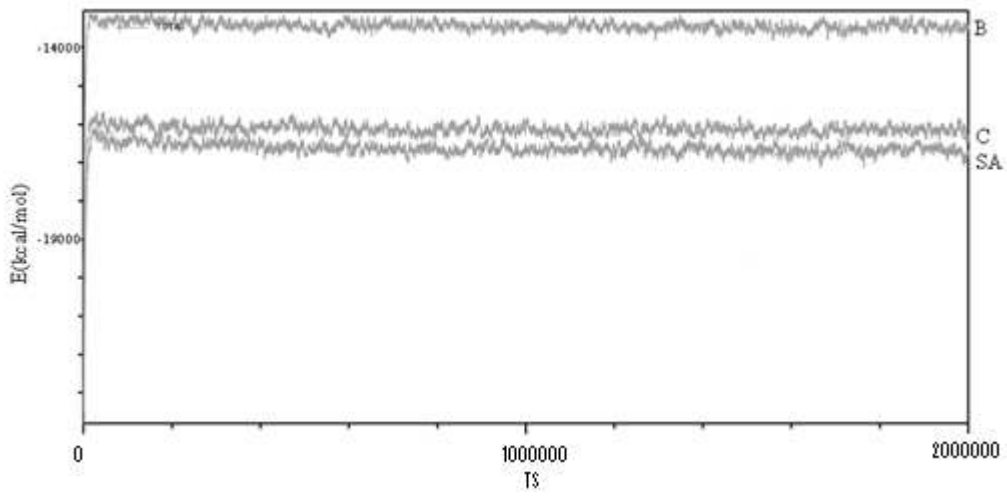

Figure-7/15: Total energy (E) of the models plotted as a function of simulation time indicated as number of time steps (TS).

Average total energy of the models during the simulation is shown in the figure-15. Though models SA and C show distant sequence similarity (table-IV) their average energy is almost equal. Similarly sequential most similar models SA and B are showing a large difference in their total energy. The increased RMSF of the residues of model B coincides with the maximum total energy among the models. It shows the structure B is

less stable than other two models. It may be noted that the energy of a molecule is more dependent on its structure and various interactions than its sequence.

Chapter 5

5. Conclusion

Human immunodeficiency virus (HIV) is a retrovirus that causes acquired immunodeficiency syndrome. The life cycle of HIV inside the human host is complex and precise consisting many macromolecular interactions and activations. Each function is the window to next function performing role of molecular check point. Inhibiting one step effects the next impeding the cycle of viral replication and function.

The structural basis for cyclin T1 interaction with Tat and TAR is still unclear. Cyclin T1 is believed to interact with Tat through metal ions stabilized by essential cysteine residues found in both proteins [94, 95]. Since the cysteine-rich and hydrophobic regions of the free Tat protein are highly flexible, it seems likely that they undergo conformational rearrangements during assembly of the ternary complex with cyclin T1. The TAR RNA binding motif shows less structural dynamics and more conformational stability (Figure-14b, Table-V). This may be the requirement for steady binding to the RNA element. Again any change in core region shows decreased in stability. Taking the model B which had more deviations in its core region (21-47) is least stable as it has maximum total energy (figure-15). The reverse is true for the model SA where lesser RMSD across the residues in this region shows higher stability of protein when energy is considered. The role of the hydrogen interactions for maintaining functional and structural viability of the protein is also clearly demonstrated (Table-V). Our study defines three regions in Tat protein structure. The first region consists of residues 1 to 47 and vital for various catalytic function of the protein. This region is characterized by minimal substitution or substitution by near group residues (Table-II, III), presence of structural motifs for molecular recognition (Figure-10, 11) and high motion (Figure-13). The second region (aa 48-59), which is responsible for RNA binding, shows no residual variation (Table-II) and minimal molecular dynamics motion (Figure-6b, c). The region is quite stable with many hydrogen interactions (Table-V). In the third region (aa 60-86) the residual interactions takes the central role in place of residue itself (Table-VI). The region has a stable conformation with least residual fluctuations (Figure-13).

Our results indicate that the presence of hydrogen interactions appreciably affects the system dynamics, providing stabilization to some regions of the protein structure, while causing increased fluctuations in other areas where the residues are not stabilized by it. In addition to this residual position and the role of the domain in function of the

protein can be suitably correlated to the residual motion during molecular dynamics simulation. The study also explains the pre binding stability of the active site of Tat protein which is crucial for its intended function. Structural and sequential analysis of the macromolecules both with time and conditional variance is needed for measuring the state of variability of each molecule. Then relating these to the interaction data will certainly point out the conserved sequential stages the viral progression. Then these stages can be examined for inhibitory suitability by different ligands or other variables.

Acknowledgements

This work was done in the Bioinformatics Infrastructure Facility (BIF) available in the Department of Biotechnology and Medical Engineering at National Institute of Technology, Rourkela, funded by the Department of Biotechnology, India.

6. References

1) Greene W.C. "The molecular biology of human immunodeficiency virus type 1 infection" N Engl J Med 324(5) (1991): 308-317

2) Kao S.Y., Calman A.F., Luciw P.A., Peterlin B.M. "Anti-termination of transcription within the long terminal repeat of HIV-1 by Tat gene product" Nature 330 (1987): 489-493

3) Gottlieb M.S. "Pneumocystis pneumonia-Los Angeles. 1981" Am J Public Health 96 (2006): 980–982

4) Barré-Sinoussi F., Chermann J.C., Rey F., Nugeyre M.T., Chamaret S., Gruest J., Dauguet C., Axler-Blin C., Vézinet-Brun F., Rouzioux C., Rozenbaum W., Montagnier L. "Isolation of a T-lymphotropic retrovirus from a patient at risk for acquired immune deficiency syndrome (AIDS)" Science 20; 220(4599) (1983 May): 868-871.

5) Popovic M., Sarngadharan M.G., Read E. and Gallo R.C. "Detection, isolation, and continuous production of cytopathic retroviruses (HTLV-III) from patients with AIDS and pre-AIDS" Science 224 (4648) (1984): 497-500

6) Coffin J., Haase A., Levy J.A., Montagnier L., Oroszlan S., Teich N., Temin H., Toyoshima K., Varmus H., Vogt P. "What to call the AIDS virus?" Nature 321 (1986): 1-7

7) Levy J.A. "Pathogenesis of human immunodeficiency virus infection" Microbiol Rev 57(1) (1993): 183-289

8) International Committee on Taxonomy of Viruses. 61.0.6. Lentivirus. National Institutes of Health.

9) Smith J. A., Daniel *R.* "Following the path of the virus: the exploitation of host DNA repair mechanisms by retroviruses". ACS Chem Biol 1 (4) (2006): 217-26.

10) Ho D.D., Pomerantz R.J., Kaplan J.C. "Pathogenesis of infection with human immunodeficiency virus" N Engl J Med 317(5) (1987): 278-86

11) Landmarks of HIV genome,webpage,
http://www.hiv.lanl.gov/content/sequence/HIV/MAP/landmark.html

12) Göttlinger HG. "HIV-1 Gag: a Molecular Machine Driving Viral Particle Assembly and Release." HIV Sequence Compendium 2001 (2003). 2-28 Edited by: Kuiken C, Foley B, Hahn B, Marx P, McCutchan F, Mellors JW, Wolinsky S, Korber B. Published by: Theoretical Biology and Biophysics Group, Los Alamos National Laboratory, Los Alamos, NM, LA-UR 02-2877

13) Ashorn P., McQuade T.J., Thaisrivongs S. “An inhibitor of the protease blocks maturation of human and simian immunodeficiency viruses and spread of infection” Proc Natl Acad Sci USA 87 (1990): 7472-7476.

14) Kwong P.D., Wyatt R., Robinson J., Sweet R., Sodroski J. and Hendrickson W. “Structure of an HIV-1 gp120 envelope glycoprotein in complex with the CD4 receptor and a neutralizing humanantibody” Nature 393 (1998): 649–59

15) Karn J. “Tat, a novel regulator of HIV transcription and latency” HIV Sequence Compendium 2000 (2000): 2-18

16) Zapp M.L., Green M.R. “Sequence-specific RNA binding by the HIV-1 Rev protein” Nature 342 (1989): 714-716

17) Yu Q., Landau N. R., and König R. “Vif and the Role of Antiviral Cytidine Deaminases in HIV-1 Replication” HIV Sequence Compendium 2004 (2004): 2-14

18) Piguet V.and TronoV. “A Structure-function Analysis of the Nef Protein of Primate Lentiviruses” HIV Sequence Compendium 2004 (2004): 2-28

19) Mansky L.M. and Temin H.M. “Lower in vivo mutation rate of Human Immunodeficiency Virus type 1 than that predicted from the fidelityof purified reverse transcriptase” J. Viro. 69 (8) (1995): 5087–5094

20) Leitner T., Kumar S. and Albert J. “Tempo and mode of nucleotide substitutions in *gag* and *env* gene fragments in Human Immunodeficiency Virus type 1 populations with a known transmission history” J. Viro 71(6) (1997): 4761–4770

21) Bernardi G., Olofsson B., Filipski J., Zerial M., Salinas J., Cuny G., Menunier-Rotival M., and Rodier F. “The mosaic genome of warmblooded Vertebrates” Science 228 (1985): 953–958

22) Robertson D.L., Hahn B.H., Sharp P.M. "Recombination in AIDS viruses". J Mol Evol. 40 (3) (1995): 249-259

23) Osmanov S., Pattou C., Walker N., Schwardlander B., Esparza J. “WHO-UNAIDS Network for HIV Isolation and Characterization. Estimated global distribution and regional spread of HIV-1 genetic subtypes in the year 2000” Acquir. Immune. Defic. Syndr. 29 (2) (2002): 184-190

24) Perrin L., Kaiser L., Yerly S. “Travel and the spread of HIV-1 genetic variants” Lancet Infect Dis. 3 (1) (2003): 22-27

25) Carr, J. K., Foley, B. T., Leitner, T., Salminen, M., Korber, B. and McCutchan, F. (1998). “Reference Sequences Representing the Principal Genetic Diversity of HIV-1 in

the Pandemic" in Los Alamos National Laboratory (ed.): HIV Sequence Compendium Los Alamos, New Mexico*:* Los Alamos National Laboratory: *10-19.*

26) Wainberg M.A." HIV-1 subtype distribution and the problem of drug resistance" AIDS. 18 (2004): S63-S68

27) Spira S., Wainberg M.A., Loemba H., Turner D. and Brenner B.G. **"**Impact of clade diversity on HIV-1 virulence, antiretroviral drug sensitivity and drug resistance" J. Antimicro Chemotherapy 51(2003): 229-240

28) Thomson M.M., Perez-Alvarez L. and Najera R. "Molecular epidemiology of HIV-1 genetic forms and its significance for vaccine development and therapy". Lancet Infect. Dis. 2 (8) (2002): 461-471

29) Novitsky V., Rybak N., McLane M.F., Gilbert P., Chigwedere P., Klein I., Gaolekwe S., Chang S. Y., Peter T., Thior I., Ndung'u T., Vannberg F., Foley B.T., Marlink R., Lee T. H., and Essex M. "Identification of Human Immunodeficiency Virus Type 1 Subtype C Gag-, Tat-, Rev-, and Nef-Specific Elispot-Based Cytotoxic T-Lymphocyte Responses for AIDS Vaccine Design" J Virol. 75(19) (2001): 9210–9228

30) Ndung'u T., Renjifo B., and Essex M. "Construction and Analysis of an Infectious Human Immunodeficiency Virus Type 1 Subtype C Molecular Clone" J Virol. 75(11)(2001): 4964–4972

31) Daniel M.D., King N.W., Letvin N.L., Hunt R.D., Sehgal P.K., Desrosiers R.C. "A new type D retrovirus isolated from macaques with an immunodeficiency syndrome". Science 223 (4636) (1984): 602–5.

32) Kurth R. and Norley S. "Why don't the natural hosts of SIV develop simian AIDS?" J. NIH Res. 8 (1996): 33-37

33) Baier M., Dittmar M.T., Cichutek K., Kurth R. "Development of vivo of genetic variability of simian immunodeficiency virus" Proc. Natl. Acad. Sci. U.S.A. 88 (18) (1991): 8126–30.

34) Berkhout B. "Structural features in TAR RNA of human and simian immunodeficiency viruses: a phylogenetic analysis" Nucleic Acids Res. 11 (1993): 27–31

35) Jaeger J.A., SantaLucia J. Jr., and Tinoco I.Jr. "Determination of rna structure and Thermodynamics", Annu. Rev. Biochem. 62 (1993):255-87

36) Uhlenbeck O.C., Pardi A., and Feigon J. "RNA Structure Comes of Age" Cell 90(1997)833–840

37) Westhof E. and Auffinger P. “RNA Tertiary Structure, Encyclopedia of Analytical Chemistry” R.A. Meyers (Ed.) John Wiley & Sons Ltd, Chichester, 2000: 5222–5232

38) Batey R.T., Sagar M.B. and Doudna J.A. “Structural and energetic analysis of RNA recognition by a universally conserved protein from the signal recognition particle” J. Mol. Biol. 255 (2001):229-46

39) Hermann T. and Westhof E. “Rational Drug Design and High-Throughput Techniques for RNA Targets” Combinatorial Chemistry & High Throughput Screening 3 (2000): 219-234

40) Batey R.T., Rambo R.P., Doudna J.A. “Tertiary Motifs in RNA Structure and Folding” Angew Chem Int Ed Engl.38 (1999):2326-2343

41) Kessler M., Mathews M.B. “Premature termination and processing of human immunodeficiency virus type 1-promoted transcripts” J Virol 66(1992): 4488-4496

42) Zhang J., Tamilarasu N., Hwang S., Garber M.E., Huq I., Jones K.A., Rana T.A. “HIV-1 TAR RNA Enhances the Interaction between Tat and Cyclin T1” J Biol Chem 275 (2000):34314-34319

43) Dingwall C., Ernberg I., Gait M.J., Green S.M., Heaphy S., Karn J., Lowe A.D., Singh M., Skinner M.A., Valerio R. “Human immunodeficiency virus 1 Tat protein binds transactivation-responsive region (TAR) RNA in vitro’’ Proc Natl Acad Sci USA 86 (1989):6925-6929

44) Weeks K.M., Ampe C., Schultz S.C., Steitz T.A., Crothers D.M. “Fragments of the HIV-1 Tat protein specifically bind TAR RNA” Science 249 (1990):1281-1285

45) Bayer P., Kraft M., Ejchart A., Westendrop M., Frank R., Rosch P. “Structural studies of HIV-1 Tat protein” J Mol Biol 247(1995): 529-535

46) Metzger A.U., Bayer P., Willbold D., Hoffmann S., Frank R.W., Goody R.S., Rösch P. “The interaction of HIV-1 Tat (32-72) with its target RNA: a fluorescence and nuclear magnetic resonance study” Biochem Biophys Res Comm 241 (1997): 31-36.

47) Ruben S., Perkins A., Purcell R., Joung K., Sia R., Burghoff R., Haseltine W.A., Rosen C.A. “Structural and functional characterization of human immunodeficiency virus Tat protein” J Vir 63 (1989):1-8

48) Churcher M.J., Lamont C., Hamy F., Dingwall C., Green S.M., Lowe A.D., Butler P.J.G., Gait M.J., Karn J. “High affinity binding of TAR RNA by the human immunodeficiency type-1 Tat proteinrequires base-pairs in the RNA stem and amino acid residues flanking the basic region” J Mol Biol 230 (1993): 90–110

49) Willbold D., Rosin-Abersfeld R., Sticht H., Frank R., Rosch P. “Structure of the equine infectious anemia virus Tat Protein” Science 264 (1994):1584–1587

50) Olsen G.L., Edwards T.E., Deka P., Varani G., Sigurdsson S.T., Drobny G.P. “Monitoring tat peptide binding to TAR RNA by solid-state” Nucleic Acids Res 33 (2005): 3447–3454

51) Mujeeb A., Bishop K., Peterlin B.M., Turck C., Parslowtllli T.G., James T.L. “NMR structure of a biologically active peptide containing the RNA-binding domain of human immunodeficiency virus type 1 Tat” Proc Nati Acad Sci USA 91 (1994): 8248-8252

52) Cornelissen M., Van Den Burg R., Zorgdrager F., Lukashov V., Goudsmit J. “pol gene diversity of five Human Immunodeficiency Virus type 1 subtypes: evidence for naturally occurring mutations that contribute to drug resistance, limited recombination patterns, and common ancestry for subtypes B and D” J Vir71 (1997): 6348–6358

53) Mu Y., Stock G., “Conformational dynamics of RNA-peptide binding: a molecular dynamics simulation study” Biophys J 90 (2006): 391–399

54) Pantano S., Tyagi M., Giacca M., Carloni P. “Molecular dynamics simulations on HIV-1 Tat” Eur Biophys J 33 (2004): 344–351

55) Reyes C.M., Nifosi R., Frankel A.D., Kollman P.A. “Molecular dynamics and binding specificity analysis of the Bovine Immunodeficiency Virus BIV Tat-TAR complex” Biophys J 80 (2001): 2833–2842

56) Niffosi R., Reyes C.M. “Molecular dynamics studies of the HIV1 TAR and its complex with arginamide” Nucleic Acids Res 28 (2000): 4944-4955

57) Cavalli-Sforza L.L. and Edwards A.W.F. ″Phylogenetic analysis: Models and estimation procedures". Evol. 21 (3) (1967): 550-570

58) Penny D., Hendy M.D. and Steel M.A. “Progress with methods for constructing evolutionary trees” Trends in Ecology and Evolution 7 (1992): 73-79

59) Yang Z. “PAML: a program package for phylogenetic analysis by maximum likelihood” Computer Applications in BioSciences 13 (1997): 555-556

60) Edwards A.W.F., and Cavalli-Sforza, L.L. “A method for cluster analysis” Biometrics 211965(1965): 362-375

61) Zwickl D.J., Hillis D.M. "Increased taxon sampling greatly reduces phylogenetic error". Systematic Biology 51 (2002): 588-598.

62) Blomberg S.P., Garland T. Jr, Ives A.R. "Testing for phylogenetic signal in comparative data: behavioral traits are more labile". Evolution 57 (2003): 717-745.

63) Zhang Y. and Skolnick J. "The protein structure prediction problem could be solved using the current PDB library" Proc Natl Acad Sci USA 102 (4) (2005): 1029-1034
64) Bowie J.U., Luthy R., Eisenberg D. "A method to identify protein sequences that fold into a known three-dimensional structure". Science 253 (5016) (1991): 164-170
65) Marti-Renom M.A., Stuart A.C., Fiser A., Sanchez R., Melo F., Sali A. "Comparative protein structure modeling of genes and genomes" Annu Rev Biophys Biomol Struct 29 (2000): 291-325
66) Reddy C.H., Vijayasarathy K., Srinivas E., Sastry G.M., Sastry G.N. "Homology modeling of membrane proteins: A critical assessment" Computational Biology and Chemistry 30 (2006): 120–126
67) Sali A. and Blundell T.L. Comparative protein modelling by satisfaction of spatial restraints. J. Mol. Biol. 234 (1993.): 779–815
68) Nayeem A., Sitkoff D.and Krystek S. "A comparative study of available software for high-accuracy homology modeling: From sequence alignments to structural models" Protein Sci. 15 (2006): 808-824
69) Chung S.Y., Subbiah S. "A structural explanation for the twilight zone of protein sequence homology" Structure 4 (1996): 1123–27.
70) Alder B. J., Wainwright T. E. "Studies in Molecular Dynamics. I. General Method". J. Chem. Phys. 31 (2) (1959): 459
71) Sanbonmatsu K. Y. And Tung C.S. "High performance computing in biology: multimillion atomsimulations of nanoscale systems" J Struct Biol. 157(3) (2007): 470–480.
72) McQuarrie D., "Statistical Mechanics" Harper & Row, New York, 1976
73) Chandler D. Introduction to Modern Statistical Mechanics, Oxford University Press, New York, 1987
74) Wilde R. E. and Singh S. "Statistical Mechanics, Fundamentals and Modern Applications" John Wiley & Sons, Inc, New York, 1998
75) http://en.wikipedia.org/wiki/Molecular_dynamics
76) Finn R.D., Mistry J., Schuster-Böckler,B., Griffiths-Jones S., Hollich V., Lassmann T., Moxon S., Marshall M., Khanna A., Durbin R., Eddy S.R., Sonnhammer E.L.L., Bateman A. "Pfam: clans, web tools and services" Nucleic Acids Res Database 34 (2006): D247-D251

77) Thompson J.D., Higgins D.G., Gibson T.J. "CLUSTAL W: improving the sensitivity of progressive multiple sequence alignment through sequence weighting, position-specific gap penalties and weight matrix choice" Nucleic Acids Res 22 (1994): 4673–4680

78) Rice P., Longden I., Bleasby A. "EMBOSS: The European Molecular Biology Open Software Suite" Trends in Genetics 16 (2000): 276—277

79) Laskowski R.A., Rullmannn J.A., Macarthur M.W., Kaptein R., Thornton J.M. "AQUA and PROCHECK-NMR: programs for checking the quality of protein structures solved by NMR" J Biomol NMR 8 (1996): 477-486

81) Lehtonen J.V., Still D.J., Rantanen V.V., Ekholm J., Björklund D., Iftikhar Z., Huhtala M., Repo S., Jussila A., Jaakkola J., Pentikäinen O., Nyrönen T., Salminen T., Gyllenberg M., Johnson M. "BODIL: a molecular modeling environment for structure-function analysis and drug design" J Comput Aided Mol Des 18 (2004): 401-419

82) Eswar N., Marti-Renom M. A., Webb B., Madhusudhan M.S., Eramian D., Shen M., Pieper U., Sali A. "Current Protocols in Bioinformatics" John Wiley & Sons, Inc. (2000) : 5.6.1-5.6.30

83) Kale L., Skeel R., Bhandarkar M., Brunner R., Gursoy A., Krawetz N., Phillips J., Shinozaki A., Varadarajan K., Schulten K. "NAMD2: greater scalability for parallel molecular dynamics" J Comput Phys151 (1999): 283–312

84) Pettersen E.F., Goddard T.D., Huang C.C., Couch G.S., Greenblatt D.M., Meng E.C . and Ferrin T.E. "UCSF Chimera - A Visualization System for Exploratory Research and Analysis" J Comput Chem 25(13) (2004): 1605-1612

85) Jorgensen W.L., Chandrasekhar J., Madura J.D., Impey R.W., Klein M.L. "Comparison of simple potential functions for simulating liquid water" J Chem Phys 79 (1983): 926–935.

86) Darden T., York D., Pedersen L. "Particle-mesh Ewald—ann_log(n) method for Ewald sums in large systems" J Chem Phys 98 (1993): 10089–10092

87) MacKerell A.D., Bashford D., Bellott M., Dunbrack R.L., Evanseck J.D., Field M.J., Fischer S., Gao J., Guo H., Ha S., Joseph-McCarthy D., Kuchnir L. "All-atom empirical potential for molecularmodeling and dynamics studies of proteins" J Phys Chem B 102 (1998): 3586–3616

88) Nose S. "A unified formulation of the constant-temperature molecular-dynamics methods" J Chem Phys 81 (1984): 511–519

89) Hoover W.G. “Canonical dynamics: equilibrium phase-space distributions” Phys Rev A 31 (1985): 1695–1697

90) Brunger A. “X-PLOR, Version 3.1: A System for X-Ray Crystallography and NMR” Yale University, New Haven, CT (1992)

91) Friedler A., Friedler D., Luedtke N. W., Tor Y. and Loyter A., Gilon C. J. Biol Chem *275* (2000): 23783–23789

92) Kuppuswamy M., Subramanian T., Srinivasan A., Chinnadurai G. “Multiple functional domains of Tat, the trans-activator of HIV-1, defined by mutational analysis” Nucleic Acids Res17 (1989): 3551–3561

93) Churcher M.J., Lamont C., Hamy F., Dingwall C., Green S.M., Lowe A.D., Butler P.J.G., Gait M.J., Karn J. “High affinity binding of TAR RNA by the human immunodeficiency type-1 Tat protein requires base-pairs in the RNA stem and amino acid residues flanking the basic region” J Mol Biol 230 (1993): 90–110

94) Bieniasz P.D., Grdina T.A., Bogerd H.P., Cullen B.R. “Recruitment of a protein complex containing Tat and cyclin T1 to TAR governs the species specificity of HIV-1 Tat” EMBO J 17 (1998): 7056–7065

95) Garber M.E., Wei P., Jones K.A. “The interaction between HIV-1 Tat and human cyclin T1 requires zinc and a critical cysteine residue that is not conserved in the murine CycT1 protein” Cold Spring Harbor Symp Quant Biol 63 (1998): 371–380

96) Saladino A.C, Xu Y. and Tang P. “Homology modeling and molecular dynamics simulations of transmembrane domain structure of human neuronal nicotinic acetylcholine receptor” Biophysical Journal (2005): 1009–1017

97) Herce H.D. and Garcia A.E. “Molecular dynamics simulations suggest a mechanism for translocation of the HIV-1 TAT peptide across lipid membranes” PNAS 107(2007): 20805–20810

98) Gumbart J. and Schulten K. “Molecular Dynamics Studies of the Archaeal Translocon” Biophysical Journal 90 (2006): 2356–2367

99) Bastug T., Kuyucak S. “Molecular dynamics simulations of calcium binding in gramicidin A” Chemical Physics Letters 424 (2006): 82–85

100) Amaro R.E., Swift R.V., McCammon J.A. “Functional and structural insights revealed by molecular dynamics simulations of an essential RNA editing ligase in Trypanosoma brucei” PLoS Neglected Tropical Diseases1 (2007): 1-10

101) Isralewitz B., Izrailev S. and Schulten K. **"**Binding pathway of retinal to bacterio-opsin: a prediction by molecular dynamics simulations" Biophysical Journal 73 (1997): 2972-2979

102) Kosztin D., Izrailev S., Schulten K. "Unbinding of retinoic acid from its receptor studied by steered molecular dynamics" Biophysical Journal 76 (1999): 188–197

103) Fengler A., Mrestani-Klaus C., Reinhold D., renger S., Ansorge S., Faust J., Neubert K. and Brandt W. "Determination of the solution conformation of HIV-1 Tat(1-9) peptides by means of molecular dynamics simulations considering NMR data and docking studies into an active site model of DP IV" J. Mol. Model 4 (1998): 200 – 210

104) Pantano S., Tyagi M., Giacca M. and Carloni P. "Amino acid modification in the HIV-1 Tat basic domain: insights from molecular dynamics and in vivo functional studies" J. Mol. Biol. 318 (2002): 1331–1339

105) Phillips J.C., Braun R., Wang W., Gumbart J., Tajkhorshid E., Villa E., Chipot C., Skeel R.D., Kale L., Schulten K. "Scalable Molecular Dynamics with NAMD" J Comput Chem 26 (2005): 1781–1802

106) Ewald P P. "Evaluation of optical and electrostatic lattice potentials" Ann. Phys. Leipzig 64 1921: 253-287

Appendix1

Codes for structural modeling

```
# Homology modeling by the automodel class

from modeller import *                    # Load standard Modeller classes

from modeller.automodel import *    # Load the automodel class


log.verbose()      # request verbose output

env = environ()  # create a new MODELLER environment to build this model in


# directories for input atom files

env.io.atom_files_directory = './:../atom_files'


a = automodel(env,

                    alnfile  = '1tbc_c.ali',        # alignment filename

                    knowns   = '1tbc',              # codes of the templates

                    sequence = 'C')                 # code of the target

a.starting_model= 1                 # index of the first model

a.ending_model  = 1                 # index of the last model

                                    # (determines how many models to calculate)

a.make()                            # do the actual homology modeling
```

Appendix2

Codes for molecular dynamics simulation

1) Psfgen file

```
package require psfgen

topology top_all27_prot_lipid.inp

pdbalias residue HIS HSE

pdbalias atom ILE CD1 CD

segment U {pdb 1tbc_cp.pdb}

coordpdb 1tbc_cp.pdb U

guesscoord

writepdb 1tbc_c.pdb

writepsf 1tbc_c.psf
```

2) Water sphere file

```
### Script to immerse ubiquitin in a sphere of water just large enough
### to cover it

set molname 1tbc_c

mol new ${molname}.psf
mol addfile ${molname}.pdb

### Determine the center of mass of the molecule and store the coordinates
set cen [measure center [atomselect top all] weight mass]
set x1 [lindex $cen 0]
set y1 [lindex $cen 1]
set z1 [lindex $cen 2]
set max 0
```

```
### Determine the distance of the farthest atom from the center of mass
foreach atom [[atomselect top all] get index] {
  set pos [lindex [[atomselect top "index $atom"] get {x y z}] 0]
  set x2 [lindex $pos 0]
  set y2 [lindex $pos 1]
  set z2 [lindex $pos 2]
  set dist [expr pow(($x2-$x1)*($x2-$x1) + ($y2-$y1)*($y2-$y1) + ($z2-$z1)*($z2-$z1),0.5)]
  if {$dist > $max}  {set max $dist}
  }

mol delete top

### Solvate the molecule in a water box with enough padding (15 A).
### One could alternatively align the molecule such that the vector
### from the center of mass to the farthest atom is aligned with an axis,
### and then use no padding
package require solvate
solvate ${molname}.psf ${molname}.pdb -t 15 -o del_water

resetpsf
package require psfgen
mol new del_water.psf
mol addfile del_water.pdb
readpsf del_water.psf
coordpdb del_water.pdb

### Determine which water molecules need to be deleted and use a for loop
### to delete them
set wat [atomselect top "same residue as {water and ((x-$x1)*(x-$x1) + (y-$y1)*(y-$y1)
+ (z-$z1)*(z-$z1))<($max*$max)}"]
set del [atomselect top "water and not same residue as {water and ((x-$x1)*(x-$x1) + (y-
$y1)*(y-$y1) + (z-$z1)*(z-$z1))<($max*$max)}"]
set seg [$del get segid]
```

```
set res [$del get resid]
set name [$del get name]
for {set i 0} {$i < [llength $seg]} {incr i} {
  delatom [lindex $seg $i] [lindex $res $i] [lindex $name $i]
  }
writepsf ${molname}_ws.psf
writepdb ${molname}_ws.pdb

mol delete top

mol new ${molname}_ws.psf
mol addfile ${molname}_ws.pdb
puts "CENTER OF MASS OF SPHERE IS: [measure center [atomselect top all] weight
mass]"
puts "RADIUS OF SPHERE IS: $max"
mol delete top
```

3) Minimization file

```
#############################################################
## JOB DESCRIPTION                                         ##
#############################################################

# Minimization of tat in a Water Box

#############################################################
## ADJUSTABLE PARAMETERS                                   ##
#############################################################

structure          ../common/b/1tbc_b_wb.psf
coordinates        ../common/b/1tbc_b_wb.pdb

set temperature    310
set outputname     b_min
firsttimestep      0

#############################################################
## SIMULATION PARAMETERS                                   ##
#############################################################
# Input
paraTypeCharmm          on
parameters          ../common/b/par_all22_prot_cmap.inp
temperature         $temperature
```

```
# Force-Field Parameters
exclude             scaled1-4
1-4scaling          1.0
cutoff              12.
switching           on
switchdist          10.
pairlistdist        13.5

# Integrator Parameters
timestep              1.0  ;# 2fs/step
nonbondedFreq         2
fullElectFrequency    4
stepspercycle         20

# Periodic Boundary Conditions
cellBasisVector1    47.6   0.   0.
cellBasisVector2     0.   42.7  0.
cellBasisVector3     0.    0   36.9
cellOrigin          -5.0  -0.85  5.3
wrapAll             on

# PME (for full-system periodic electrostatics)
PME                 yes
PMEGridSizeX        48
PMEGridSizeY        45
PMEGridSizeZ        40

# Constant Pressure Control (variable volume)
useGroupPressure      yes ;# needed for rigidBonds
useFlexibleCell       no
useConstantArea       no

langevinPiston            on
langevinPistonTarget  1.01325 ;#  in bar -> 1 atm
langevinPistonPeriod  100.
langevinPistonDecay   50.
langevinPistonTemp    $temperature

constraints on
consref    ../common/b/1tbc_b_wb.pdb
conskfile ../common/b/1tbc_b_wb.pdb
conskcol B
constraintScaling 1
# Output
outputName          $outputname

restartfreq         500     ;# 500steps = every 1ps
dcdfreq             500
```

```
xstFreq           250
outputEnergies     100
outputPressure     100

#############################################################
## EXECUTION SCRIPT                                        ##
#############################################################

# Minimization
minimize           3000
reinitvels         $temperature
```

4) Parameter file for simulation

```
#############################################################
## JOB DESCRIPTION                                         ##
#############################################################

# Simulation of Tat

#############################################################
## ADJUSTABLE PARAMETERS                                   ##
#############################################################

structure          ../common/c/1tbc_c_wb.psf
coordinates        ../common/c/1tbc_c_wb.pdb
outputName         c_eq1

# set temperature    310

# Continuing a job from the restart files
if {1} {
set inputname       c_min
binCoordinates     $inputname.restart.coor
binVelocities      $inputname.restart.vel  ;# remove the "temperature" entry if you use this!
extendedSystem           $inputname.xsc
}
firsttimestep      0

#############################################################
## SIMULATION PARAMETERS                                   ##
#############################################################

# Input
paraTypeCharmm          on
parameters         ../common/c/par_all22_prot_cmap.inp

# NOTE: Do not set the initial velocity temperature if you
# have also specified a .vel restart file!
```

```
# temperature         $temperature

wrapWater           on
wrapAll             on

# Force-Field Parameters
exclude             scaled1-4
1-4scaling          1.0
cutoff              12.
switching           on
switchdist          10.
pairlistdist        13.5


# Integrator Parameters
timestep            1.0  ;# 2fs/step
nonbondedFreq       2
fullElectFrequency  4
stepspercycle       20



# Constant Temperature Control
langevin            on    ;# do langevin dynamics
langevinDamping     5     ;# damping coefficient (gamma) of 5/ps
langevinTemp        310
langevinHydrogen    no    ;# don't couple langevin bath to hydrogens


# Constant Pressure Control (variable volume)
useGroupPressure      yes ;# needed for 2fs steps
useFlexibleCell       no  ;# no for water box, yes for membrane
useConstantArea       no  ;# no for water box, yes for membrane

langevinPiston        on
langevinPistonTarget  1.01325 ;#  in bar -> 1 atm
langevinPistonPeriod  100.
langevinPistonDecay   50.
langevinPistonTemp    310

constraints on
consref    ../common/c/1tbc_c_wb.pdb
conskfile ../common/c/1tbc_c_wb.pdb
conskcol B
constraintScaling 1.0
```

```
restartfreq          500     ;# 500steps = every 1ps
dcdfreq              500
xstFreq              250
outputEnergies       100
outputPressure       100


#############################################################
## EXECUTION SCRIPT                                        ##
#############################################################

run 500000 ;# 50ps
```